Doctoral thesis

Functional-morphological relationships of vasopressin in the macaque neuroendocrine system

2025

Akito Otubo

Graduate School of Natural Science and Technology
(Doctor's Course)
OKAYAMA UNIVERSITY

Contents

General Introduction

Arginine vasopressin (AVP), an anti-diuretic hormone, is released, not only into the bloodstream, but also into the central nervous system where, in mammals, it has been shown to be important for stress coping, aggression, courtship behavior, learning, bonding, and various socio-sexual behaviors [1]. These diverse functions mediated by AVP are determined by the morphological characteristics of AVP-producing neurons, including their projection areas and vesicular architecture. AVP neurons are classified into magnocellular neurons, which mediate systemic endocrine functions, and parvocellular neurons, which mediate more localized neuroendocrine roles. Magnocellular AVP neurons are located in the supraoptic nucleus (SON) and paraventricular nucleus (PVN) of the hypothalamus [2], and their axons project primarily *via* the internal layer of the median eminence (ME) to the posterior pituitary (Figure GI.1). In contrast, parvocellular AVP neurons are located in the PVN and project into extrahypothalamic areas where AVP and/or other co-packaged molecules regulate brain function as neuromodulators [3]. Notably, a population of parvocellular AVP neurons projects to the external layer of the ME and co-expresses corticotropin-releasing factor (CRF) alongside AVP [4] (Figure GI.1). Under stressed conditions, AVP and CRF are released from the external layer of the ME into the pituitary portal vessels, where they act on corticotropes in the anterior pituitary to synergistically enhance adrenocorticotropic hormone (ACTH) secretion [5-11]. By activating the hypothalamic–pituitary–adrenal (HPA) axis, this mechanism elicits physiological responses—such as increases in blood glucose and blood pressure, enhanced lipolysis, and suppression of inflammatory processes—that collectively bolster the organism's resilience to stress. Since AVP neurons exhibit diverse functions depending on their projection targets and peptide

release modalities, their morphological characteristics are believed to be closely linked to their functional roles. However, studies on the functional–morphological relationships of AVP in the neuroendocrine system have predominantly relied on rodent models, leaving these relationships in primates, including humans, largely unexplored.

In the present study, the functional–morphological relationships of AVP in the primate neuroendocrine system were investigated using the Japanese macaque monkey (*Macaca fuscata*), which is relatively close to humans. This study focused on two aspects: (ⅰ) the intracellular localization and functional significance of AVP and CRF in the neuroendocrine system, and (ⅱ) the morphological characterization of AVP neurons.

In Chapter 1, I investigated whether AVP and CRF co-localize within dense-core vesicles in parvocellular neurons and are co-released under stress. Although rodent studies have shown that these peptides coexist within the same granules and synergistically enhance ACTH secretion [4, 12-14], this phenomenon has not yet been validated in primates. To address this gap, fluorescence immunohistochemistry and immunoelectron microscopy were combined to analyze the granular co-localization of AVP and CRF in the external layer of the macaque ME.

In Chapter 2, I quantitatively assessed the ultrastructural morphological features of magnocellular and parvocellular AVP neurons using immunoelectron microscopy and examined their relationship to functional diversity. In addition to measuring secretory granule diameters, vesicular glutamate transporter 2 (VGLUT2) and glutamate localization were investigated to evaluate whether AVP neurons exhibit glutamatergic transmission. These two distinct vesicle architectures are thought to support the functional versatility of the primate AVP system.

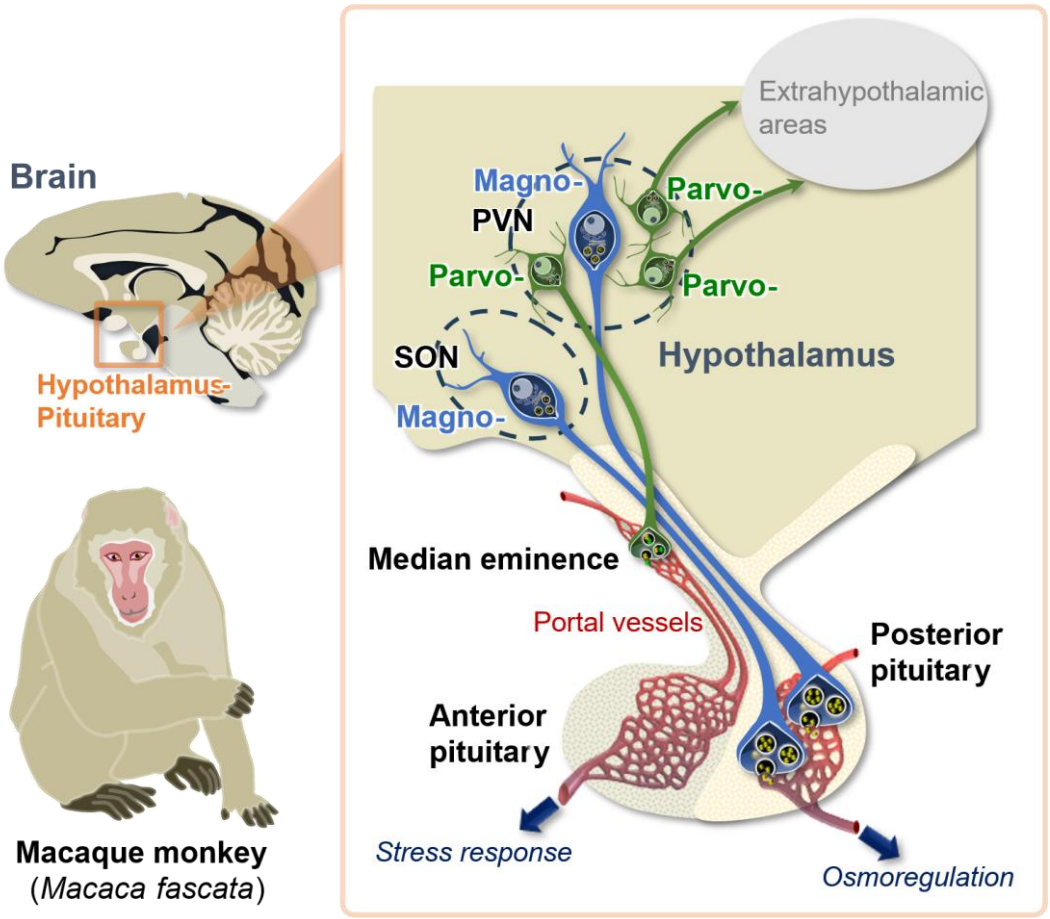

Figure GI.1 Schematic diagram of magnocellular and parvocellular neurons in the hypothalamic–pituitary axis of the macaque. Magnocellular neurons (blue) are located in the supraoptic nucleus (SON) and paraventricular nucleus (PVN) of the hypothalamus, and their axons project *via* the internal layer of the median eminence (ME) to the posterior pituitary. In contrast, parvocellular neurons (green) are located in the PVN and project into extrahypothalamic areas. A population of parvocellular neurons projects to the external layer of the ME and release vasopressin and corticotropin-releasing factor into the pituitary portal vessels. Magno-, magnocellular neuron; Parvo-, parvocellular neuron.

Chapter 1

The intracellular localization and functional significance of AVP/CRF in the macaque neuroendocrine system

Vasopressin gene products are colocalized with corticotropin-releasing factor within neurosecretory vesicles in the external zone of the median eminence of the Japanese macaque monkey (*Macaca fuscata*)

Summary

Arginine vasopressin (AVP), when released into portal capillaries with corticotropin-releasing factor (CRF) from terminals of parvocellular neurons of the hypothalamic paraventricular nucleus (PVN), facilitates the secretion of adrenocorticotropic hormone (ACTH) in stressed rodents. The *AVP* gene encodes a propeptide precursor containing AVP, AVP-associated neurophysin II (NPII), and a glycopeptide copeptin, although it is currently unclear whether copeptin is always cleaved from the neurophysin and whether the NPII and/or copeptin have any functional role in the pituitary. Furthermore, for primates, it is unknown whether CRF, AVP, NPII, and copeptin are all colocalized in neurosecretory vesicles in the terminal region of the paraventricular CRF neuron axons. Therefore, the cellular and subcellular relationships of these peptides in the CRF- and AVP-producing cells in unstressed Japanese macaque monkeys (*Macaca fuscata*) were investigated by fluorescence and immunogold immunocytochemistry. Reverse transcription-polymerase chain reaction analysis showed the expression of both *CRF* and *AVP* mRNAs in the monkey PVN. As expected, in the magnocellular neurons of the PVN and supraoptic nucleus, essentially no CRF-immunoreactivity could be detected in NPII-immunoreactive (AVP-producing) neurons. Immunofluorescence showed that, in the parvocellular part of the PVN, NPII was detectable in a subpopulation (approximately 39%) of the numerous CRF-immunoreactive neuronal perikarya, whereas, in the outer median eminence, NPII was more prominent (approximately 52%) in the CRF varicosities. Triple immunoelectron microscopy in the median eminence demonstrated the presence of both NPII and copeptin-immunoreactivity in dense-cored vesicles of CRF-containing axons. These results are consistent with an idea that the AVP propeptide is processed and NPII and copeptin are colocalized in hypothalamic-pituitary CRF axons in the median eminence of a primate. The CRF, AVP, and copeptin are all co-packaged in neurosecretory vesicles in monkeys and are thus likely to be co-released into the portal capillary blood to amplify ACTH release from the primate anterior pituitary.

Introduction

The hypothalamic neuroendocrine response to stress is an important survival mechanism in vertebrates. Corticotropin-releasing factor (CRF), a 41-amino-acid peptide, potently stimulates adrenocorticotropic hormone (ACTH) secretion from the anterior pituitary when released into the portal capillaries of the median eminence (ME) from terminals of parvocellular neurons of the hypothalamic paraventricular nucleus (PVN) [15-17]. The release of arginine vasopressin (AVP) into portal capillary plasma results in a stronger ACTH response than that obtained with CRF alone, because of the synergistic action of CRF and AVP to induce ACTH release [5-11]. A population of CRF neurons in the PVN can co-secrete AVP, and both peptides are secretagogues for ACTH in mammals, including rats [18] and humans [13]. Furthermore, the expression of the *AVP* gene in CRF neurons is increased in stressed conditions [19, 20]. Translation of the *AVP* gene results in the formation of a propeptide which is cleaved to release the AVP hormone, but which also contains the AVP-associated neurophysin (NP) II, and a glycopeptide copeptin [21-23]. The NPII has the important function of binding/stabilizing the AVP [24], although the function of the copeptin and when and if it is proteolytically cleaved from the NPII is currently unclear [25]. In many mammals, including rats and humans, ultrastructural immunocytochemistry demonstrates that CRF and AVP are copackaged into the same dense-cored neurosecretory vesicles (dcv) in the CRF-positive ($^{+}$) and AVP^{+} subpopulation of fibers in the ME, indicating that they are almost certainly co-released into the portal capillary blood [14, 26]. The concentration of AVP in the pituitary portal vessels increases when animals are stressed or are subjected to adrenalectomy [27]. Although, in unstressed mice, very few parvocellular neurons are doubly positive for CRF and AVP, severe stress or adrenalectomy significantly increases the ratio of double positive cells (to half) [12]. However, at least in primates, it is unknown whether CRF, AVP, and the AVP-associated NPII and copeptin can all be detected in dcv in both the cell bodies and terminal region of the CRF neuron axons. Furthermore, any clear evidence for the function of the secreted copeptin is currently lacking [25]. This present study provides the first evidence in the hypothalamus of unstressed Japanese macaque monkeys (*Macaca fuscata*) that CRF, AVP, and the AVP-associated NPII and copeptin are all co-packaged within the dcv, and therefore that the AVP precursor protein undergoes proteolysis during the passage of the dcv from the CRF perikarya to the ME.

Materials and Methods

Ⅰ.1 | Animals

Three male (2–9 years old, weight 2.4–12.6 kg) and four female (9–11 years old, weight 7.2–8.2 kg) Japanese macaque monkeys (*Macaca fuscata*) were used in this study. Monkeys were maintained in a temperature-controlled (22–24 °C) room under a daily photoperiod of 12:12 hour light/dark cycle (lights off at 8:00 p.m.). These animals were checked and shown to be free of specific pathogens. Food and water were available *ad libitum*. All animals were kept in individual cages. The housing and experimental protocols followed the guidelines of the Ministry of Education, Culture, Sports, Science, and Technology (MEXT) of Japan, and were in accordance with the Guide for the Care and Use of Laboratory Animals prepared by Okayama University (Okayama, Japan), by Kyoto Prefectural University of Medicine (Kyoto, Japan), and by Kansai Medical University (Osaka, Japan). All efforts were made to minimize animal suffering and reduce the number of animals used in this study.

Ⅰ.2 | Experimental Procedures

Ⅰ.2.1 RNA Extraction and Reverse Transcription (RT)-PCR

One male and two female monkeys were anaesthetized with an overdose of sodium pentobarbital (50–90 mg/kg body weight), transcardially perfused with physiological saline, and euthanized by blood loss. The hypothalamus and cerebral cortex (temporal lobe) were quickly removed and frozen with powdered dry ice and stored at −80 °C until RNA extraction. Brains were sectioned at 100 μm thickness with a cryostat (CM3050 S, Leica, Nussloch, Germany). Sections were then dissected at −20 °C into 2–3 mm square tissue fragments containing either the PVN or temporal cortex. Total RNA was extracted using an illustra RNAspin Mini RNA isolation kit (GE Health Care Bioscience, Piscataway, NJ, USA) according to the manufacturer's protocol. The concentration of total RNA was measured using a NanoDrop Lite (Thermo Fisher Scientific, Waltham, MA, USA). First-strand cDNA was synthesized from 200 ng of total RNA with random primers using Omniscript RT kit (QIAGEN, Hilden, Germany). The RT-PCR conditions for target genes and glyceraldehyde-3-phosphate dehydrogenase (GAPDH) as an internal control are shown in Table 1.1. The PCR amplicons were electrophoresed on 2% agarose gels. RT-PCR studies were repeated three times using independently extracted RNA samples from different animals. Consistent results were obtained from each run.

Ⅰ.2.2 Tissue Preparation for Microscopic Analysis

Two male and two female monkeys were anaesthetized with an overdose of sodium pentobarbital (50–90 mg/kg body weight), and transcardially perfused with physiological saline followed by 4% paraformaldehyde (PFA) in 0.1 M phosphate buffer (PB, pH7.4). Hypothalami were immediately removed and immersed in either 4% PFA in 0.1 M PB (for immunofluorescence) or 4% PFA + 0.1% glutaraldehyde (for electron microscopic studies) for 16–24 hours at 4 °C. The fixed tissue was then sectioned in the coronal plane at 30–60 μm thickness with a Linear-Slicer (PRO10, Dosaka EM, Kyoto, Japan).

Ⅰ.2.3 Immunofluorescence

The sections were rinsed with phosphate-buffered saline (PBS) containing 0.3% Triton X-100 (PBST) three times for 5 minutes each. After blocking nonspecific binding with 1% normal goat serum and 1% BSA in PBST for 30 minutes at room temperature, the sections were incubated with primary rabbit antisera directed against CRF (1:20,000 dilution) or copeptin (1:10,000 dilution) and with a mouse monoclonal anti-AVP-NPⅡ antibody (1:1,000 dilution) for 4–5 days at 4 °C. The rabbit polyclonal antiserum against rat/human copeptin was generated in-house and previously characterized by Western blot analysis in rats [28]. The copeptin$_{7\text{-}14}$ (ATQLDGPA) fragment, used as an antigen to produce the copeptin antiserum, is well conserved in mammals. It is identical in rats [29], mice [30], macaque monkeys [GenBank accession numbers XM_005568487.2 (*Macaca fascicularis*) and XM_011741311.2 (*Macaca nemestrina*)], common marmosets [GenBank accession number XM_002747402.2 (*Callithrix jacchus*)], and humans [29]. Thus, the antiserum appears to be appropriate for use in various mammalian species including primates. The mouse monoclonal NPⅡ (PS41) antibody has previously shown to be specific for AVP neurons in rodents [31, 32]. The rabbit polyclonal antiserum against rat/human CRF (PBL rC70), which was kindly donated by Wylie Vale, has been characterized elsewhere [33]. It was directed against the rat form of CRF, which is identical to the human form, and has also been characterized in non-human primates [34]. Alexa Fluor 546-linked anti-mouse IgG (Molecular Probes, Eugene, OR, USA) and Alexa Fluor 488-linked anti-rabbit IgG (Molecular Probes) were used for detection at 1:1,000 dilution. Immunostained sections were viewed by confocal laser scanning microscopy (FluoView 1000, Olympus, Tokyo, Japan). The antibodies used in this study are showed in Table 1.2.

The proportion of AVP(NPⅡ)-containing neurons in the CRF^{+} neuronal population of the PVN was analyzed. For each of four or five 30 μm-thick PVN sections at ×200 magnification per animal (n = 4 monkeys; two females, two males), unit areas (630 × 630 μm^2) in the PVN containing CRF-positive neurons were analyzed. In total, 87

unit areas from 17 sections were analyzed. The number of the immunoreactive cells with clearly visible transected nuclei was counted.

The co-expression ratio of the immunoreactivity for CRF/NP Ⅱ was also determined in sections of the ME. For each of the four to five 30 μm-thick sections per animal (n = 4 monkeys; two females, two males), unit areas (50 × 50 μm^2) were analyzed at ×400 magnification to determine CRF/NP Ⅱ-immunoreactivity. In total 74 unit areas in the external layer and 60 unit areas in the internal layer from 17 sections were analyzed. The optical density of the immunostaining of CRF (green), NP Ⅱ (magenta), and the merged images (green, magenta, and white) were all determined by preparing black-white images that were converted from each immunofluorescent micrograph by use of ImageJ software (ImageJ 1.52a; National Institutes of Health, Bethesda, MD, USA). The optical density of the background labelling was estimated by comparison with similar areas of the control sections (Figure 1.1). Each threshold optical density was determined by normalizing the data to those of the control sections. The CRF/NP Ⅱ-immunoreactive-fiber pixel density was semi-quantitated as the average pixel density in both the external and internal layers of the ME. The percentage of co-expression ratio was calculated, according to the following formula: *[pixel density of CRF-immunoreactivity (green) + pixel density of NP Ⅱ-immunoreactivity (magenta) – pixel density of the merged image (including all green, magenta, and white signals)]/pixel density of NP Ⅱ-immunoreactivity (magenta) • 100.*

Ⅰ.2.4 Post-Embedding Immunoelectron Microscopy

Slices of PFA + glutaraldehyde-fixed tissues containing the ME were dehydrated through increasing concentrations of methanol, flat-embedded in LR Gold resin (Electron Microscopy Sciences, Hatfield, PA, USA), and polymerized under UV lamps at −25 °C for 24 hours. Ultrathin sections (70 nm in thickness) were collected on nickel grids coated with (or without for triple labelling) a collodion film, rinsed with PBS several times, then incubated with 2% normal goat serum and 2% BSA in 50 mM Tris(hydroxymethyl)-aminomethane-buffered saline (TBS; pH 8.2) for 30 minutes to block non-specific binding. The sections were then incubated with the rabbit polyclonal antiserum against CRF (1:5,000 dilution) or copeptin (1:100 dilution) and a 1:200 dilution of the PS41 mouse monoclonal antibody against NPII for 2 hours at room temperature. For double immunoelectron microscopy, after incubation with the primary antibodies, the sections were washed with PBS, then incubated with a 1:50 dilution of a goat antibody against rabbit IgG conjugated to 10-nm gold particles (BBI Solutions, Cardiff, UK) and a goat

antibody against mouse IgG conjugated to 15-nm gold particles (BBI Solutions) for 1 hour at room temperature.

Triple immunoelectron microscopy with antibodies against CRF, NP Ⅱ, and copeptin was performed by using the front and back of ultrathin sections mounted on nickel grids without a supporting film. First, immunocytochemistry with a pair of primary antibodies (CRF and NPII) was performed on one side of the section and detected using 15-nm (mouse) and 10-nm (rabbit) colloidal gold particles (BBI Solutions), respectively. Next, immunocytochemistry with the other primary rabbit antibody (against copeptin) was performed on the other side of the section and detected by use of 5-nm colloidal gold particles (BBI Solutions). Finally, the sections were contrasted with uranyl acetate and lead citrate and viewed using an H-7650 (Hitachi, Tokyo, Japan) or JEM-1010 (JEOL, Tokyo, Japan) electron microscope operated at 80 kV. The antibodies used in this study are showed in Table 1.2.

Quantification of labelled dcv in the different varicosities was performed. At least five electron microphotographs (photographed at 5,000× magnification; 3.6 × 3.6 μm^2) per animal (n = 4 monkeys; two males and two females) of randomized regions in the external layer of the ME were analyzed. The external layer of the ME was defined by the diameter of the dcv (~100 nm) as expected for axons derived from parvocellular neurons in the PVN [32, 35]. Labelled dcv were counted manually in immunoreactive varicosities including three or more dcv. Numbers of CRF- and NPII-specific gold particles were counted, and represented as the numbers of immunoreactive gold particles per dcv. For those varicosities in which one or more NPII-labelled dcv could be identified [*i.e.* excluding varicosities in which only CRF-immunoreactivity could be detected (CRF^+, $NPII^-$)], the proportion (%) of dcv containing both CRF- and NPII-specific gold particles, and also the proportion (%) of dcv containing either only CRF- or only NPII-specific gold particles, were calculated.

Ⅰ.3 | Statistical Analysis

The data are presented as the mean ± standard error of the mean (SEM) and were analyzed using Statcel4 software. Statistical analysis of the number of CRF- and NPII-specific gold particles was assessed using Student's t test.

Results

RT-PCR Analysis of CRF, AVP, and OXT mRNA Expression

The expressions of *CRF*, *AVP*, and *OXT* mRNAs in the PVN were examined by RT-PCR. Figure 1.2 shows that bands were detected at the expected sizes for *CRF*, *AVP*, and *OXT* genes in the PVN of both sexes. *CRF* mRNA but not *AVP* or *OXT* mRNAs was also detected in the cerebral cortex. Nearly equivalent amounts of *GAPDH* cDNA were amplified from RNA preparations among these tissues, which showed that no significant RNA degradation had occurred and a proper RT was obtained in this study.

Immunofluorescent Distribution and Co-Localization of CRF and AVP(NP Ⅱ) Neurons in the Hypothalamus

Figure 1.3 shows the topographic distribution of the neuronal components of the PVN, supraoptic nucleus, and ME derived from immunofluorescent labelling for CRF (left; green) and AVP-associated NPII (right; magenta) derived from coronal sections of the macaque hypothalamus. Neurons expressing NPII are referred to as 'AVP(NPII)' neurons.

In the PVN, a difference in size between neurons in the putative 'parvo'- and 'magnocellular' divisions of the PVN was not apparent in these primates; in both parts the immunostained neuronal perikarya appeared to be of similar size. In the magnocellular part of the PVN (PaM), essentially no CRF-immunoreactivity could be detected in the AVP(NPII)-immunoreactive neurons (Figure 1.4A). By contrast, in the medial parvocellular part of the PVN (PaPV), numerous neurons were CRF-immunoreactive and 39.0 ± 0.6% of the CRF^+ perikarya contained detectable AVP(NPII)-immunoreactivity (Figure 1.4B; *arrowheads*). Virtually all AVP(NPII)-immunoreactive neurons in the PVN also contained copeptin-immunoreactivity (Figure 1.5). The CRF^+ and $AVP(NPII)^+$ neurons were also more intermingled with magnocellular neurons in the monkey than in rodent PVN, as reported previously [34, 36]. In the SON, no neurons exhibited both AVP(NPII)- and CRF-immunoreactivity (Figure 1.3).

The immunofluorescence labelling for CRF and AVP(NPII) in the macaque ME shows the topographic distribution of the specific staining as previously reported (Figure 1.1A) [37, 38]. The internal and external zones were separated by a region in which the numerical density of immunoreactive processes was much lower (Figure 1.1A and 1.5A). A dense plexus of CRF^+ fibers was present in the external layer of the ME as reported previously [37], and analysis of the immunoreactivity suggests that 52.3 ± 1.5% of CRF^+ fibers co-expressed AVP(NPII) (Figure 1.6A; *arrowheads*). By contrast, in the internal layer of the ME, $AVP(NPII)^+$ fibers were the most prominent, and only 2.8 ± 0.3% fibers

contained both AVP(NPII)- and CRF-immunoreactivity (Figure 1.6A). Controls in which the primary antiserum was omitted showed no immunostaining in the ME (Figure 1.1).

Double immunofluorescence for AVP(NPII) and the AVP-associated copeptin showed that, as expected, most AVP(NPII)$^+$ fibers in the ME also exhibited copeptin-immunoreactivity in both the internal and external layers (Figure 1.6B). In the zone between the internal and external zones, CRF-immunoreactivity was most marked (Figure 1.6A merged) and, as in the PaPV, in only about half of the CRF-immunoreactive fibers could AVP(NPII)- or copeptin-immunoreactivity also be detected (Figure 1.6B merged).

Ultrastructural Co-Localization of CRF, AVP(NP Ⅱ), and Copeptin in Dcv

Electron microscopy showed that, in the external layer of the ME, the diameter of the dcv was approximately 100 nm as expected for axons derived from parvocellular neurons in the PVN (Figure 1.7) [32, 35]. Double immunoelectron microscopy for CRF/AVP(NPII) (Figure 1.7) showed that, in the varicosities where both immunoreactivity was present, some individual vesicles were labelled by gold particles of both 10-nm and 15-nm, demonstrating the vesicular colocalization of both CRF and AVP(NPII) (Figure 1.7A, B, B'). In some neighboring terminals, only CRF single-positive vesicles could be detected (Figure 1.7A, *asterisks* and C, C').

Quantification showed that the number of CRF-specific gold particles per dcv was 5.2 ± 0.5 (n = 1,875 dcv), and that the number of AVP(NPII)-specific gold particles per dcv was 0.2 ± 0.0 (n = 1,389 dcv). Thus, the number of CRF-specific gold particles was significantly higher than that of AVP(NPII). In addition, the percentage of dcv containing both CRF- and NPII-specific gold particles located in the AVP(NPII)-immunoreactive varicosities was 12.6 ± 1.7%. The percentage of dcv containing only CRF-specific gold particles located in the AVP(NPII)-expressing varicosities was 70.4 ± 3.1%, and containing only AVP(NPII)$^+$ was 0.6 ± 0.4%.

Double labelling also showed that, in some AVP(NPII)$^+$ varicosities, the dcv were also positive for copeptin (Figure 1.8A, B, B'). However, no immunoreactivity for AVP(NPII) or copeptin could be detected in many neighboring varicosities (Figure 1.8A, *asterisk*, C, C'). Triple immunoelectron microscopy for CRF/AVP(NPII)/copeptin confirmed that the dcv in certain neurosecretory axons contained CRF-, AVP(NPII)-, and copeptin-immunoreactivity together (Figure 1.9A, B, B'), and triple-immunopositive vesicles were frequently seen. Neighboring fibers often contained only CRF single-positive dcv (Figure 1.9A, *asterisk*, C, C'). Very few gold particles were associated with other intra-varicosity organelles, such as the mitochondria, and background labelling over

glial and endothelial elements was also extremely low. Immunoelectron microscopy studies were repeated independently at least three times using different monkeys and always produced similar results.

Discussion

This is the first report of the subcellular colocalization of CRF, the AVP-associated NPII, and copeptin (and therefore also AVP) in dcv in the hypothalamic parvocellular CRF-secreting system of a primate. The RT-PCR analysis indicated the expression of both *CRF* and *AVP* mRNAs in the monkey PVN. Earlier immunocytochemical studies have also reported that CRF and AVP can be localized to the same parvocellular neurons in the rat [14], mouse [12], and also in the human PVN [13, 26, 39]. However, although it seems likely that CRF and the other AVP precursor components (NPII and copeptin) are co-packaged within the same dcv in the primate hypothalamus, there has thus far been no anatomical evidence.

In unstressed monkeys, in the medial part of the PVN where the parvocellular perikarya from which axons terminating in the ME are located, approximately 61% CRF^+ perikarya did not contain immunodetectable amounts of NPII or copeptin (approximately 39% contained immunodetectable NPII). The internal zone of the ME contained only a few CRF fibers as expected. In the pre-terminal region between the internal and external zones of the ME, only a minority of the CRF-immunoreactive fibers contained AVP (NPII)- or copeptin-immunoreactivity and the overall amount of immunoreactivity was less marked, suggesting fewer dcv in the axons at this point. In the external zone of the ME close to the hypothalamo-pituitary capillaries, all three peptides (CRF, AVP, and copeptin) were located in about half of the axons (approximately 52% of the CRF-immunoreactive tissue was also NPII-immunoreactive). In other adjacent axons containing CRF^+ vesicles, no AVP(NPII) or copeptin could be detected. These observations are consistent with reports that, in unstressed rodents, only a minority of the CRF neurons produce significant amounts of the AVP precursor, but that either stress or adrenalectomy activates the production of AVP (and therefore the AVP precursor molecule) in the CRF neurons [12, 14]. These findings suggest that the difference in the extent to which AVP, NPII and copeptin are present in the CRF and magnocellular systems relates primarily to the proportion of the neurons that express the *AVP* gene, rather than any differences in the rate of processing of the AVP precursor. In the internal zone of the ME through which the magnocellular axons pass *en route* to the posterior pituitary, the AVP precursor has clearly been processed sufficiently to reveal prominent AVP(NPII)- and copeptin-immunoreactivity in almost all of the fibers.

Both magnocellular AVP and parvocellular CRF/AVP neurons express the prohormone convertases, PC1 and PC2 in rodents [40, 41]. In CRF/AVP neurons, the expression of PC1 is selectively regulated by glucocorticoids, but adrenalectomy has no

effect on PC1 or PC2 levels in magnocellular neurons in rats [41]. The finding that AVP(NPII)- and copeptin-immunoreactivity is somewhat more prominent in the terminal parts of the CRF-immunoreactive axons in the external ME than in their PVN perikarya could reflect the progressive proteolysis of the AVP/NPII/copeptin precursor in the CRF/AVP axons of the unstressed monkeys.

In monkeys, the axons of magnocellular AVP neurons project to the posterior pituitary *via* the internal zone of the ME, whereas other AVP-producing parvocellular neurons of the PVN have axons that project throughout the brain, including the external zone of the ME and into the spinal cord, as in other mammals [36, 42-45]. In many studies, AVP has been reported to potentiate the ACTH secretory activity of CRF at the ME level [8-10]. The expression of AVP in the parvocellular CRF neurons is increased as a result of both adrenalectomy and stress [4]. In the unstressed rat ME, approximately 44% of the CRF-immunoreactive axons and terminals were stained for AVP. By contrast, in the adrenalectomized rat ME, virtually all the CRF-immunoreactive terminals showed strong staining for AVP, suggesting that adrenalectomy causes the transformation a subpopulation of CRF^{+}/AVP^{-} axons and terminals to ones which are CRF^{+}/AVP^{+} [14]. The results indicate that, as in rodents [14], about half of the CRF neurons in monkeys maintained in unstressed conditions also produce and secrete AVP, NPII, and copeptin into the hypothalamo-portal capillaries, where both NPII and copeptin could also influence the secretion of ACTH or other anterior pituitary hormones. The *AVP* gene in CRF neurons is switched on in stressed animals [14]; the monkeys examined were not stressed, so it is unsurprising that in many CRF neurons the *AVP* gene was not expressed to a detectable extent.

In the magnocellular system, any clear evidence for a function of secreted copeptin is currently lacking [25]. However, experiments seeking a possible physiological role for either NPII or copeptin have so far been confined to the systemic circulation, and a potential role for either NPII or copeptin in the anterior pituitary has yet to be investigated. These results demonstrate that CRF, AVP(NPII), and copeptin can all be colocalized within neurosecretory vesicles in the hypothalamic CRF-secreting system. Copeptin might, therefore, play a role in the hypothalamo-pituitary adrenal axis, but further study is needed to demonstrate any such role.

In conclusion, immunofluorescence and post-embedding multiple immunoelectron microscopy revealed the subcellular colocalization of CRF, AVP-associated NPII, and copeptin in neurosecretory vesicles of around half of the hypothalamo-pituitary CRF parvocellular neurons and their axons in the ME of a macaque monkey. The results show that the CRF, AVP, and copeptin are co-packaged in

the dcv in monkeys and are thus likely to be co-released into the portal capillary blood where they may synergistically modulate ACTH release in the primate anterior pituitary.

List of Tables and Figures

Chapter 1 – Tables

Chapter 1 – Figures

Table 1.1 Primer sequences and PCR conditions

Target Gene (Accession#)	Primer Sequences (5′−3′)	Size (bp)	PCR Condition (Cycle)
CRF (XM_001094433.4)	F : CGCTGCTCTTATGCCATTT R : AACACCTGGAAACGGAAACT	162	(94°C 30 sec, 55°C 30 sec, 72°C 30 sec) × 38
AVP (XM_001115061.4)	F : TTCCTCGGCCTACTGGCCTTC R : CAGCTCTCGTCGTTGCAGCA	302	(94°C 30 sec, 55°C 30 sec, 72°C 30 sec) × 38
OXT (XM_001115045.4)	F : CCAGCGCACCCGCACCAT R : AAGCGAGTGGCGCGCTTCGA	436	(94°C 30 sec, 58°C 30 sec, 72°C 30 sec) × 35
GAPDH (XM_028828781.1)	F : GGTGAAGGTCGGAGTCAACG R : CAAAGTTGTCATGGATGACC	497	(94°C 30 sec, 58°C 30 sec, 72°C 30 sec) × 35

CRF, corticotropin-releasing factor; AVP, arginine vasopressin; OXT, oxytocin; GAPDH, glyceraldehyde-3-phosphate dehydrogenase; F, forward primer; R, reverse primer; sec, second; #, number.

Table 1.2 Primary antibodies used in this study

Antigen	Description	Source, Host Species, Cat#, or Code#	Working Dilution	Reference#	RRID
Copeptin	Synthetic peptide mapping at the amino acids 7–14 of human/mouse copeptin	Generated by our laboratory, rabbit polyclonal, CP8	1:10,000 (IF) 1:100 (EM)	[28, 46, 47]	AB_2722604
CRF	Human/rat CRF coupled to human α-globulins *via* bis-diazotized benzidine	Donated by Dr. W. Vale, rabbit polyclonal, PBL rC70	1:20,000 (IF) 1:5,000 (EM)	[33, 34, 46]	AB_2314234
NPII	Soluble proteins extracted from the posterior pituitary of the rat	ATCC, mouse monoclonal, PS41, CRL-1799	1:1,000 (IF) 1:200 (EM)	[31, 32, 45, 46]	AB_2313960

Abbreviations: ATCC, American Type Culture Collection; Cat, catalogue; CRF, corticotropin-releasing factor; EM, immunoelectron microscopy; IF, immunofluorescence; NPII, arginine vasopressin-associated neurophysin II; RRID, Research Resource Identifier; #, number.

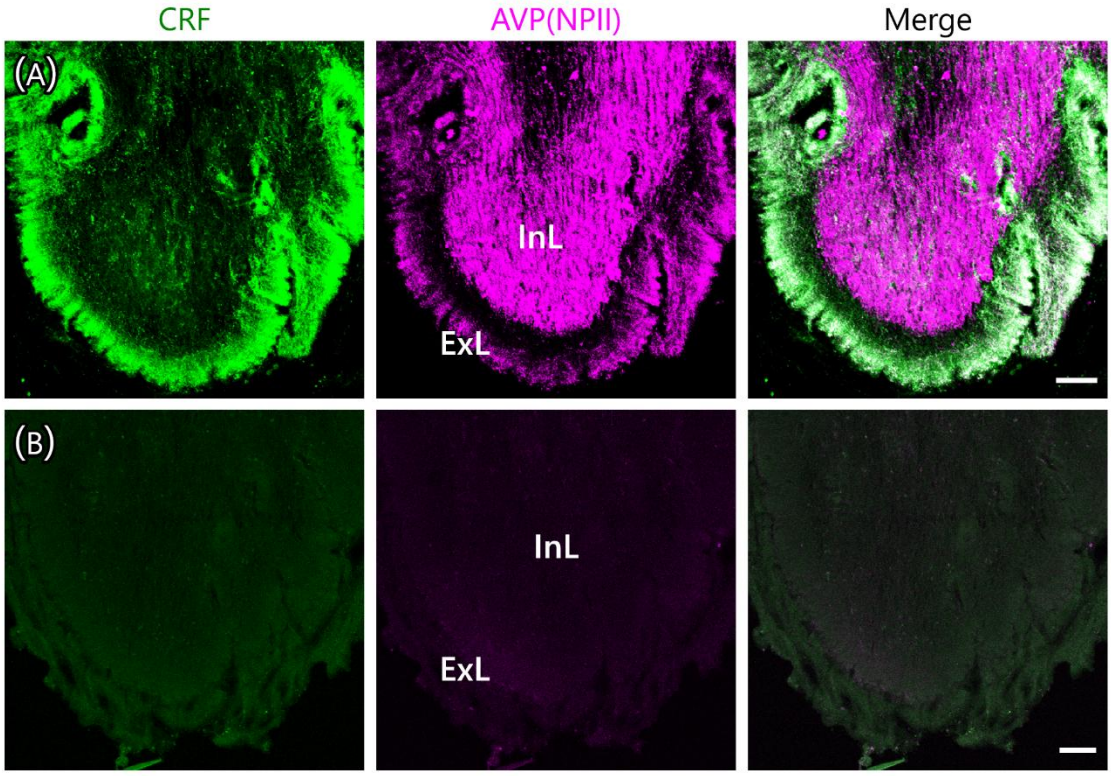

Figure 1.1 Low-magnification images of macaque median eminence (ME). (**A**) Double-label immunofluorescence for corticotropin-releasing factor (CRF) and vasopressin (AVP)-associated neurophysin (NPII) in the ME shows topographic distribution of the immunoidentified peptides as previously reported. Immunoreactivity against CRF (green) and AVP(NPII) (magenta) is merged on the right (merge). (**B**) Controls in which the primary antiserum was omitted showed no immunostaining in the ME. InL, internal layer of the median eminence; ExL, external layer of the ME. *Scale bars*, 100 µm.

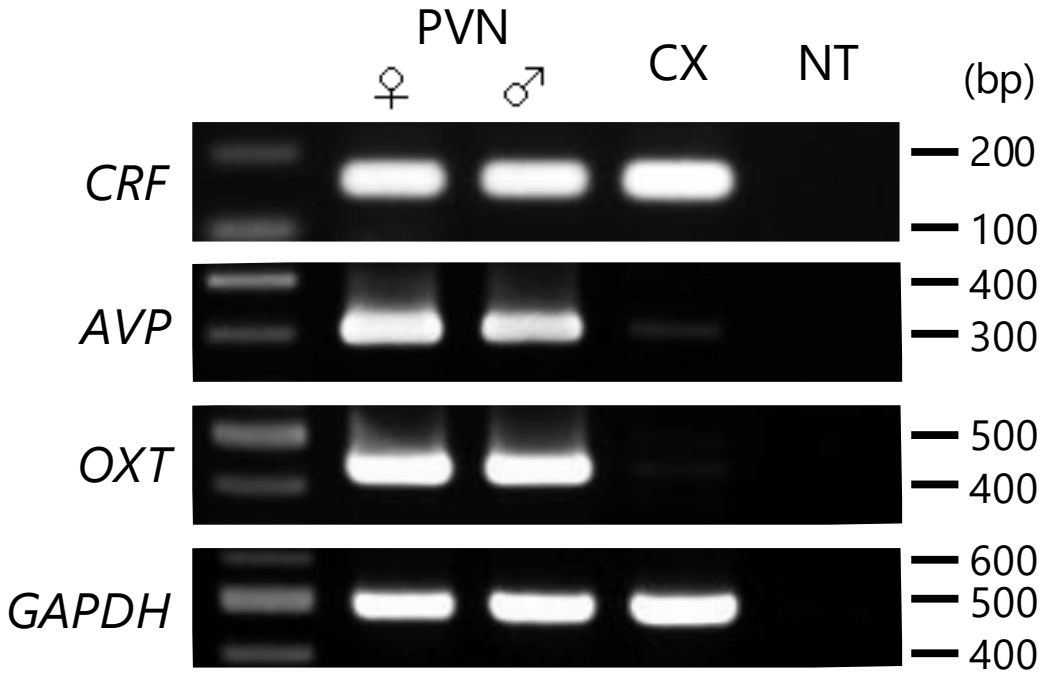

Figure 1.2 Reverse transcription (RT)-PCR analysis of corticotropin-releasing factor (*CRF*), vasopressin (*AVP*) and oxytocin (*OXT*) mRNA expression in the paraventricular hypothalamic nucleus of the hypothalamus (PVN) and cerebral cortex (CX) of monkey. RT-PCR for glyceraldehyde-3-phosphate dehydrogenase (*GAPDH*) was performed as the internal control. NT = no template control.

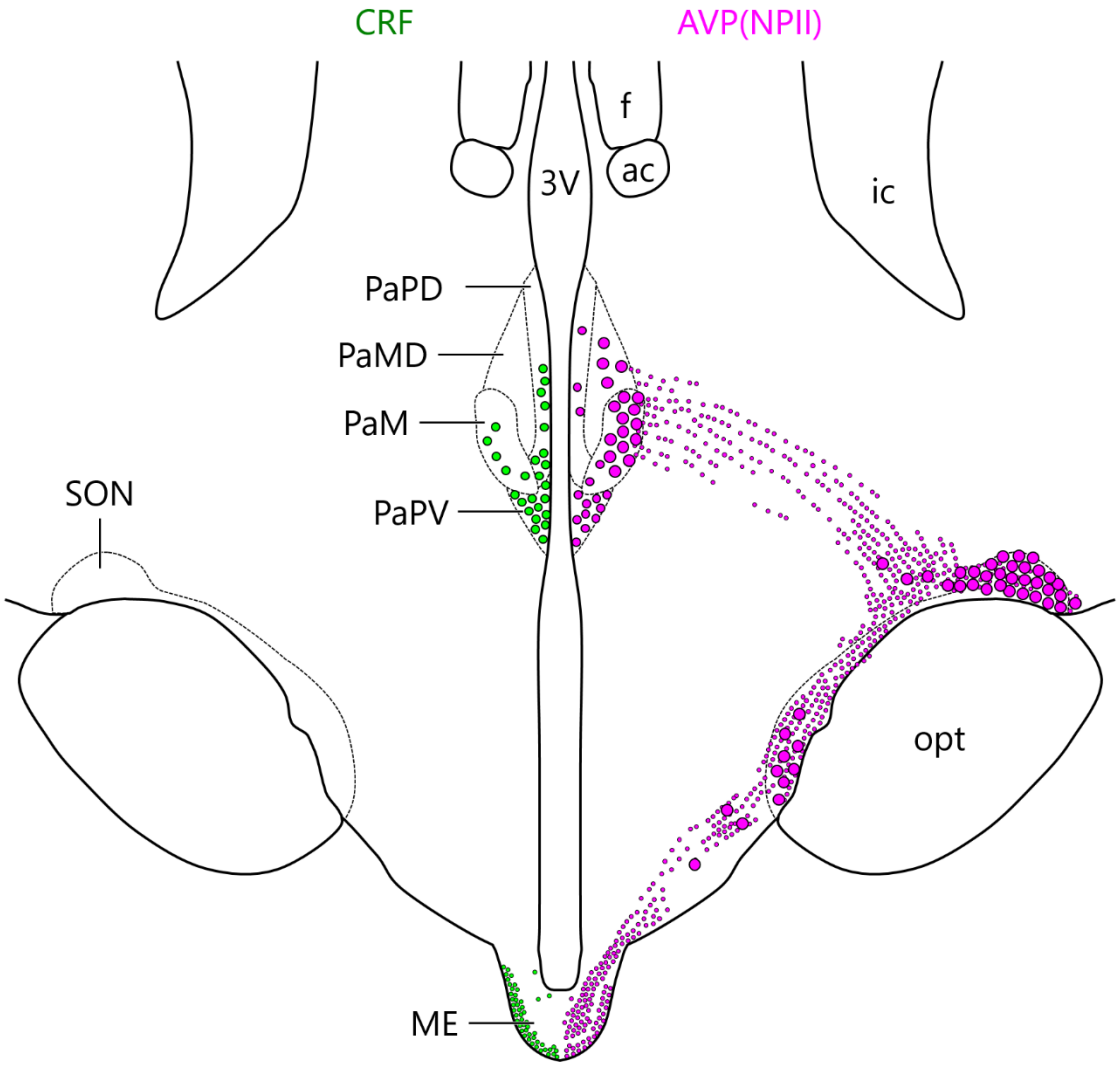

Figure 1.3 Diagram of the distribution of corticotropin-releasing factor (CRF)- and vasopressin (AVP)-associated neurophysin (NPII)-immunoreactive neurons derived from pairs of adjacent sections immunostained using anti-CRF and anti-AVP(NPII) antibodies. CRF-expressing neurons are represented by green circles; AVP-expressing neurons by magenta circles. Cell bodies are represented by large circles, and axonal projections by small circles.

Note: 3V, 3rd ventricle; ac, anterior commissure; f, fornix; ic, internal capsule; opt, optic tract; PaM, paraventricular hypothalamic nucleus, magnocellular part; PaMD, paraventricular hypothalamic nucleus, magnocellular part, dorsal division; PaPD, paraventricular hypothalamic nucleus, parvocellular part, dorsal division; PaPV, paraventricular hypothalamic nucleus, parvocellular part, ventral division; SON, supraoptic nucleus; ME, median eminence.

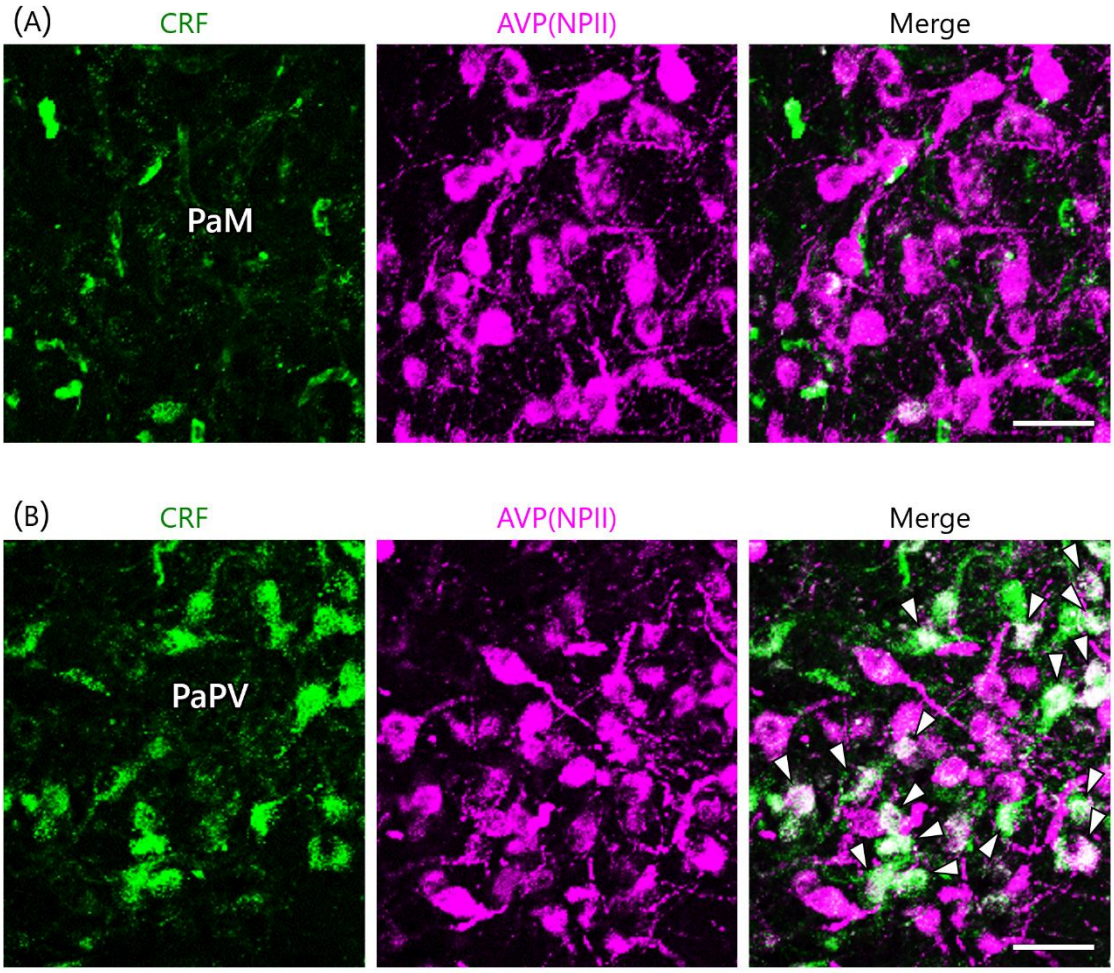

Figure 1.4 Double-label immunofluorescence for corticotropin-releasing factor (CRF) and vasopressin (AVP)-associated neurophysin (NPII) in the paraventricular nucleus of the macaque hypothalamus (PVN); PaM, paraventricular hypothalamic nucleus, magnocellular part (**A**); PaPV, paraventricular hypothalamic nucleus, parvocellular part, ventral division (**B**). Immunoreactivity against CRF (green) and AVP(NPII) (magenta) is merged on the right (merge). *Arrowheads* in (**B**) indicate perikarya doubly immunopositive for CRF and AVP(NPII) in the PaPV. *Scale bars*, 50 µm.

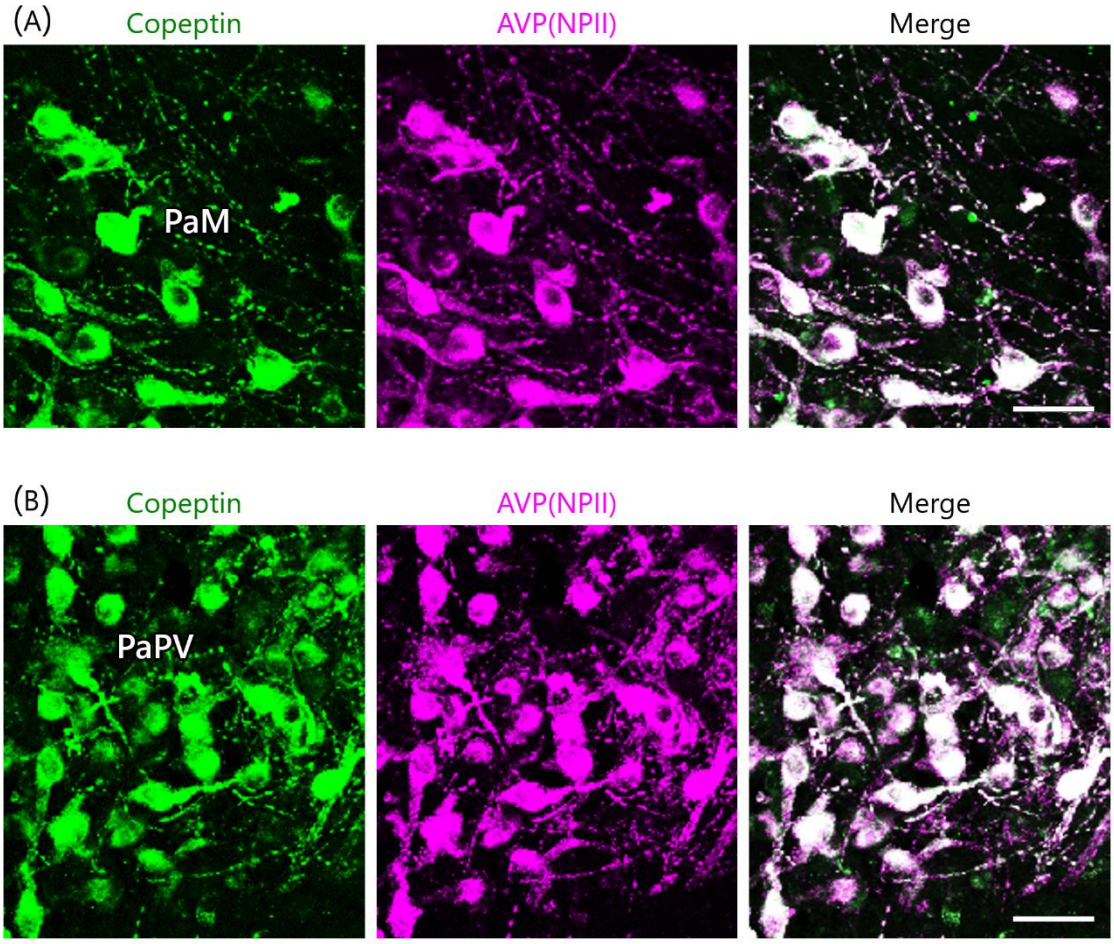

Figure 1.5 Double-label immunofluorescence for copeptin and vasopressin (AVP)-associated neurophysin (NPII) in the paraventricular nucleus of the macaque hypothalamus (PVN); PaM, paraventricular hypothalamic nucleus, magnocellular part (**A**); PaPV, paraventricular hypothalamic nucleus, parvocellular part, ventral division (**B**). Immunoreactivity against copeptin (green) and AVP(NPII) (magenta) is merged on the right (merge). The identical staining pattern between copeptin and AVP(NPII) at the cell body lecel is observed in the monkey PVN. *Scale bars*, 100 μm; 10 μm in enlarged images.

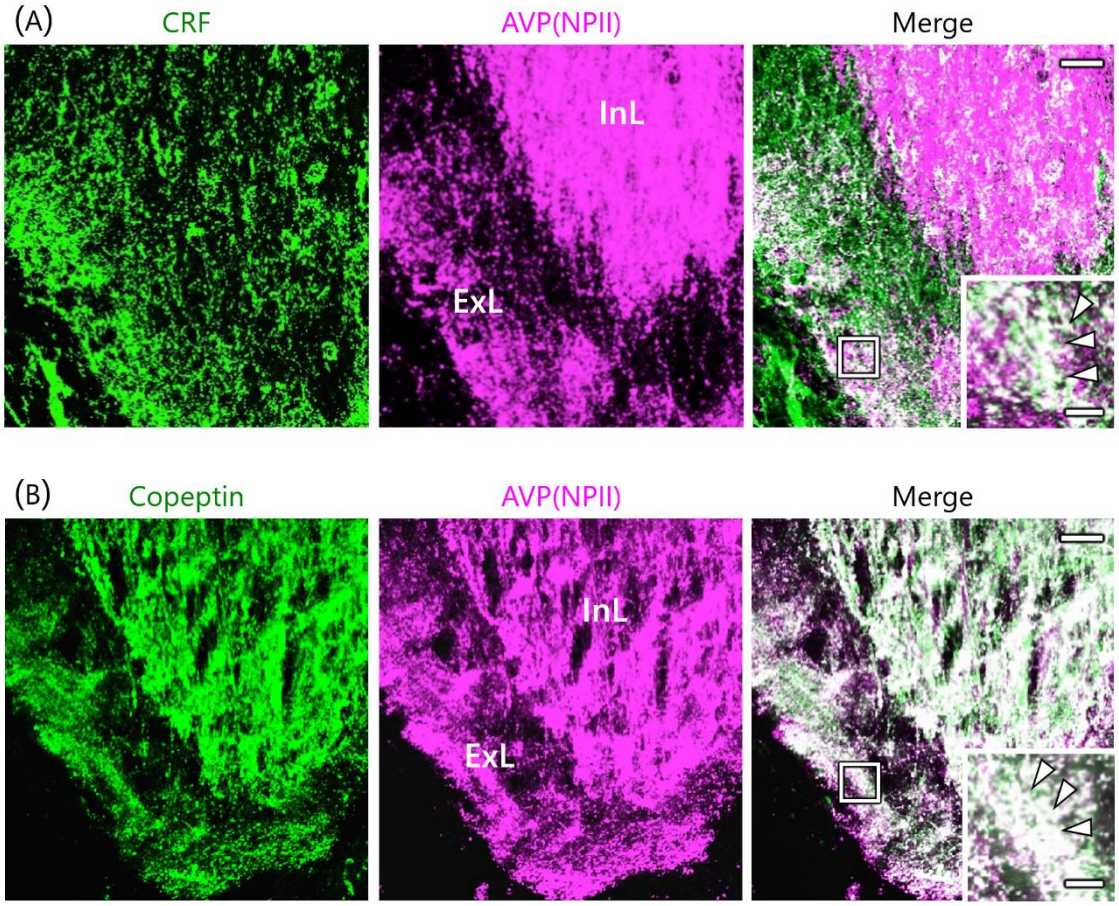

Figure 1.6 Double-label immunofluorescence for corticotropin-releasing factor (CRF) (**A**) or copeptin (**B**) and vasopressin (AVP)-associated neurophysin (NPII) in the macaque median eminence (ME). Immunoreactivity against CRF (**A**; green) or copeptin (**B**; green) and AVP(NPII) (magenta) is merged in the right (overlap white). The outlined areas in merged images are enlarged. *Arrowheads* indicate tissue doubly immunopositive for CRF or copeptin and AVP(NPII). InL, internal layer of the ME; ExL, external layer of the ME. *Scale bars*, 50 μm, and 10 μm in enlarged images.

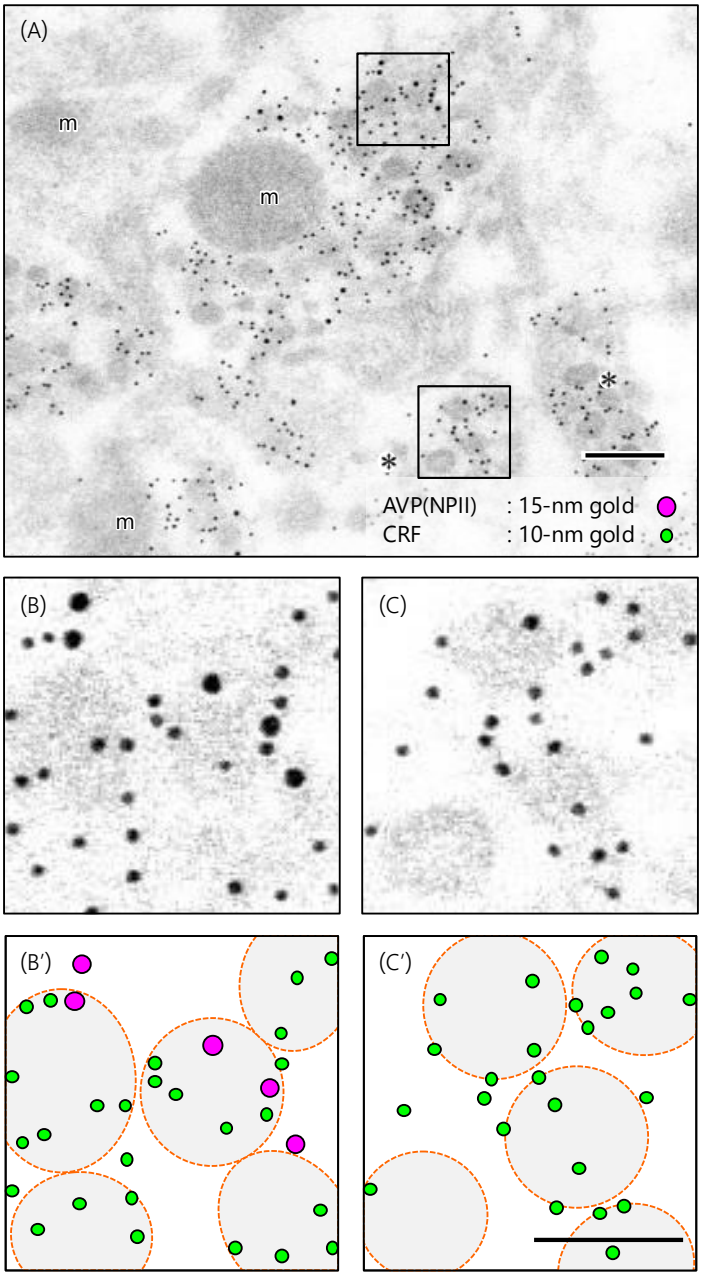

Figure 1.7 Double-label immunoelectron microscopy for vasopressin (AVP)-neurophysin (NPII) and corticotropin-releasing factor (CRF) in the external zone of the macaque median eminence. In some varicosities, numerous neurosecretory vesicles were doubly immunopositive for CRF (signalled by 10-nm gold particles) and AVP(NPII) (signalled by 15-nm gold particles). The outlined area in (**A**) is enlarged in (**B**) and (**C**). By contrast, in other neighboring varicosities no AVP(NPII)-immunoreactivity was detected (**C**). Schematic representations of the location of gold particles and neurosecretory vesicles are shown in (**B'**) and (**C'**), respectively. m, mitochondrion. *Scale bars*, 200 nm in (**A**), and 100 nm in (**C'**).

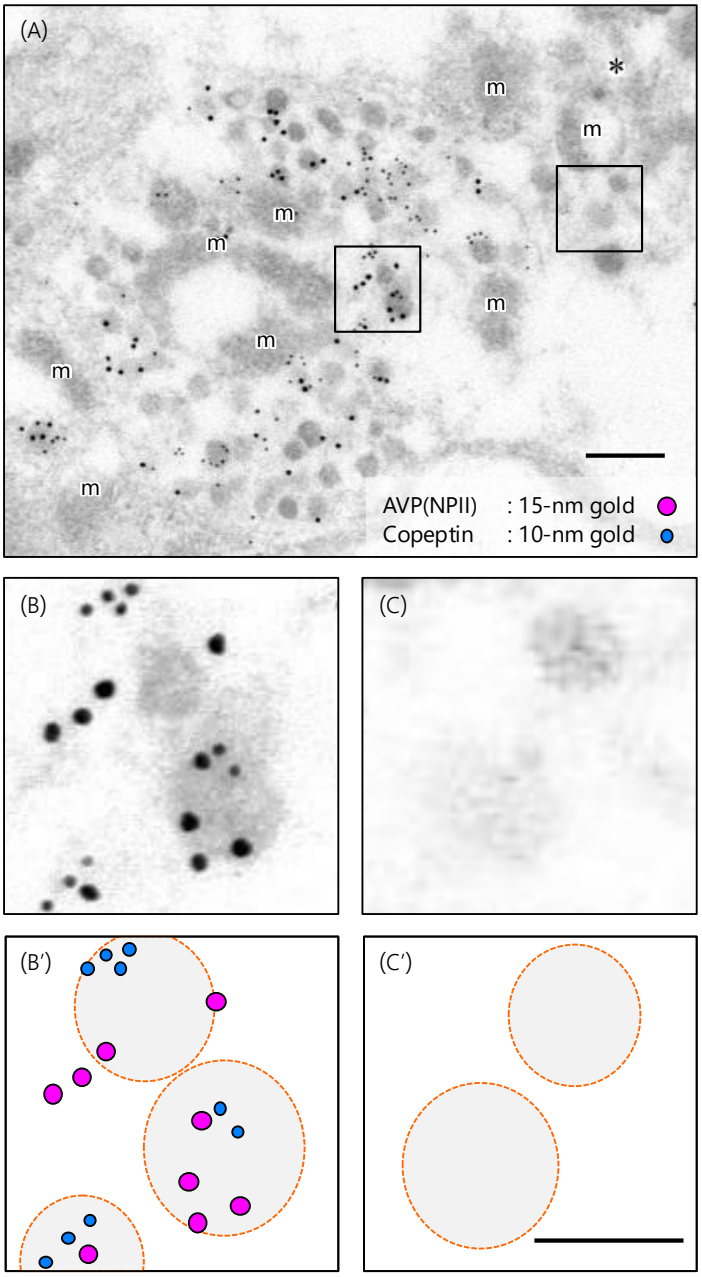

Figure 1.8 Double-label immunoelectron microscopy for vasopressin (AVP)-neurophysin (NPII) and copeptin in the external zone of the macaque median eminence. Numerous neurosecretory vesicles located in some of the varicosities were doubly immunopositive for copeptin (signalled by 10-nm gold particles) and AVP(NPII) (signalled by 15-nm gold particles). The outlined area in (**A**) is enlarged in (**B**) and (**C**). By contrast, in other neighboring varicosities no AVP(NPII)/copeptin-immunoreactivity was detected (**C**). Schematic representations of the location of gold particles and neurosecretory vesicles are shown in (**B'**) and (**C'**), respectively. m, mitochondrion. *Scale bars*, 200 nm in (**A**), and 100 nm in (**C'**).

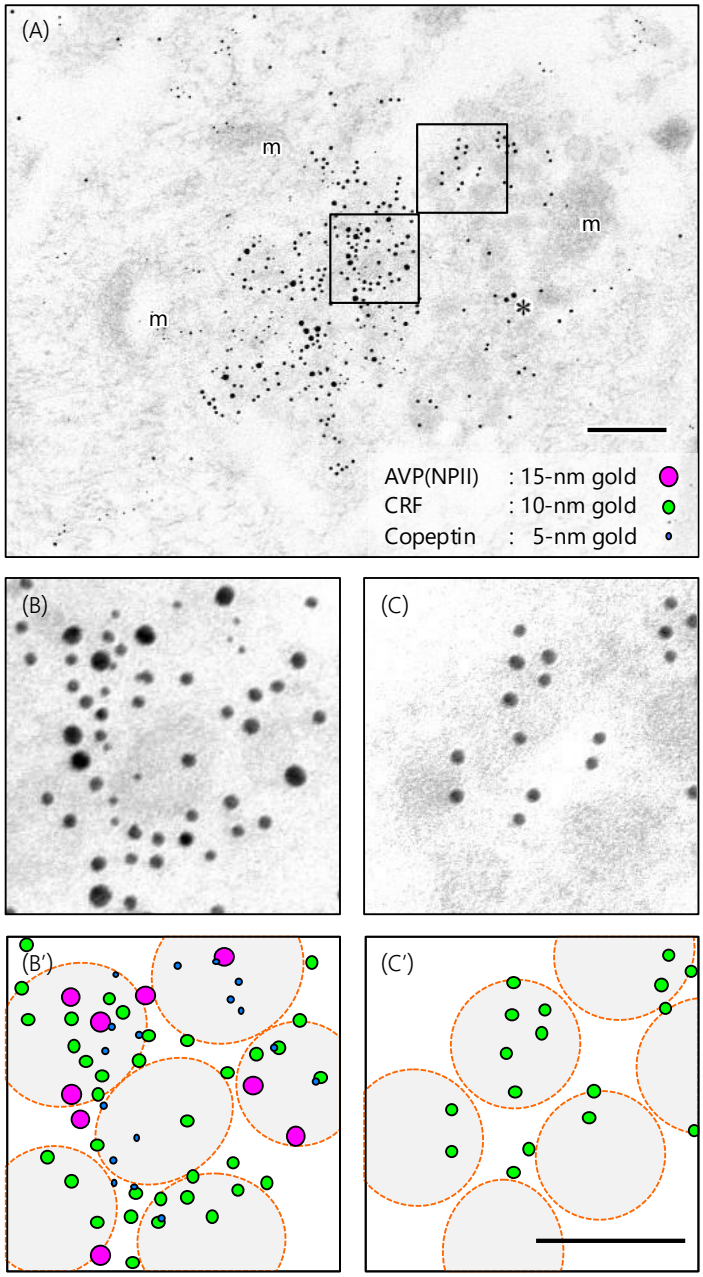

Figure 1.9 Triple-label immunoelectron microscopy for vasopressin (AVP)-neurophysin (NPII), copeptin, and corticotropin-releasing factor (CRF) in the external zone of the macaque median eminence. (**A**) AVP(NPII) (signalled by 15-nm gold particles), CRF (signalled by 10-nm gold particles), and copeptin (signalled by 5-nm gold particles) were all detected within the varicosities. (**B**) Enlarged image showing that, in some varicosities, the immunoreactivity was co-associated with single neurosecretory vesicles. By contrast, in other neighboring CRF-labelled (by 10-nm gold particles) varicosities, no AVP(NPII)/copeptin-immunoreactivity was detected (**C**). Schematic representations of the location of gold particles and neurosecretory vesicles are shown in (**B'**) and (**C'**), respectively. m, mitochondrion. *Scale bars*, 200 nm in (**A**), and 100 nm in (**C'**).

Chapter 2

The morphological characterization of AVP neurons in the macaque

Immunoelectron microscopic characterization of vasopressin-producing neurons in the hypothalamo-pituitary axis of non-human primates by use of formaldehyde-fixed tissues stored at –25 °C for several years

Summary

Translational research often requires the testing of experimental therapies in primates, but research in non-human primates is now stringently controlled by law around the world. Tissues fixed in formaldehyde without glutaraldehyde have been thought to be inappropriate for use in electron microscopic analysis, particularly those of the brain. This study reports the immunoelectron microscopic characterization of arginine vasopressin (AVP)-producing neurons in macaque hypothalamo-pituitary axis tissues fixed by perfusion with 4% formaldehyde and stored at –25 °C for several years (4–6 years). The size difference of dense-cored vesicles between magnocellular and parvocellular AVP neurons was detectable in their cell bodies and perivascular nerve endings located, respectively, in the posterior pituitary and median eminence. Furthermore, glutamate and the vesicular glutamate transporter 2 could be colocalized with AVP in perivascular nerve endings of both the posterior pituitary and the external layer of the median eminence, suggesting that both magnocellular and parvocellular AVP neurons are glutamatergic in primates. Both ultrastructure and immunoreactivity can therefore be sufficiently preserved in macaque brain tissues stored long-term, initially for light microscopy. Taken together, these results suggest that this methodology could be applied to the human post-mortem brain and be very useful in translational research.

Introduction

Studies using macaque monkeys as model non-human primates are essential because of their high applicability to human clinical research which often requires the testing of experimental therapies in primates. However, primate research is now stringently controlled by law around the world [48]. Rodents, in which research is less restricted, are often not sufficiently analogous to humans in their physiology to allow an extrapolation from rodent to human. Medical science is urged to make minimal use of animals such as primates, and basic studies on non-human primates appear to be permitted only if the work could not be carried out in any other species. Thus, although tissues from primates are often essential to achieve relevant results, there are considerable problems in their use.

Arginine vasopressin (AVP), an anti-diuretic hormone, is released, not only into the blood stream, but also into the central nervous system where, in mammals, it has been shown to be important for stress coping, aggression, courtship behavior, learning, bonding, and various socio-sexual behaviors [1]. AVP is produced mainly by magnocellular neurosecretory neurons in the supraoptic nucleus (SON) and paraventricular nucleus (PVN) of the hypothalamus [2]. The *AVP* gene encodes a precursor containing AVP, AVP-associated neurophysin II (NPII), and a glycopeptide copeptin [21-23]. The expression and release of AVP by magnocellular neurosecretory neurons in the SON and PVN are regulated by physiological conditions, including plasma osmotic pressure and blood pressure [49]. The magnocellular axons project primarily *via* the internal layer of the median eminence to the posterior pituitary where they release AVP into the systemic circulation. In addition, some parvocellular neurons in the PVN produce AVP and project into extrahypothalamic areas where the AVP and/or other co-packaged molecules regulate brain function as neuromodulators [3].

Corticotropin-releasing factor (CRF) is a strong stimulator of adrenocorticotropic hormone (ACTH) secretion from the anterior pituitary when released onto portal capillaries in the median eminence in response to the stress [15]. A population of parvocellular neurons in the anteromedial part of the PVN produces CRF and may, depending on the extent of stress, also produce AVP. Both peptides released into the hypothalamo-hypophysial portal circulation play an important synergistic role in stress resilience [4, 12-14]. Because intense AVP- and CRF-immunoreactivity have both been observed in the external layer of the macaque median eminence, the peptides are probably co-released into the portal circulation to amplify ACTH release from the primate anterior pituitary [38, 46].

In rodents, the presence of glutamate-immunoreactivity in magnocellular neuroendocrine cells of the SON suggests that AVP neurons also produce glutamate as a neurotransmitter [50, 51]. Within the neurosecretory endings of the posterior pituitary, glutamate-immunoreactivity is specifically localized to electron-lucent microvesicles with no overlap onto the dense-cored neurosecretory vesicle (dcv) population in rats [50]. Immunocytochemical co-localization of CRF and the vesicular glutamate transporter 2 (VGLUT2) in the locus coeruleus of rats suggests that the co-release of CRF and glutamate may function to regulate postsynaptic targets [52]. It is currently unclear whether glutamate has a similar or other functions in the primate hypothalamo-pituitary paraventricular AVP/CRF system.

Tissues, especially those of the brain, fixed in formaldehyde without glutaraldehyde have long been thought to be unsuitable for electron microscopic analysis by reason of the weaker cross-linking action of formaldehyde, *e.g.*, [53, 54]. The present study reports the immunoelectron microscopic characterization of AVP-producing neurons in the primate hypothalamo-pituitary axis tissue fixed by perfusion with formaldehyde and stored at –25 °C for several years. Special attention was paid to the size of dcv in AVP-producing magno- and parvocellular neurons and to the colocalization of CRF with AVP-related gene products in the dcv. The results demonstrate that immunoelectron microscopy of formaldehyde-fixed tissue can confirm the well-known size difference in dcv between magno- and parvocellular AVP neurons in Japanese macaque monkeys. Furthermore, the results indicate that in formaldehyde-fixed stored neural tissue of macaque monkeys, both AVP/CRF and VGLUT2/glutamate can be co-localized in both the magnocellular endings of the posterior pituitary and the parvocellular endings in the external layer of the median eminence.

Materials and Methods

Ⅱ.1 | Animals

Three male (2–9 years old, weight 2.3–12.6 kg) and four female (9–11 years old, weight 7.2–10.8 kg) Japanese macaque monkeys (*Macaca fuscata*) were used in this study. Macaques were maintained in a temperature-controlled (22–24 °C) room under a daily photoperiod of 12:12 hour light/dark cycle (lights off at 8:00 p.m.). These animals were checked and shown to be free of specific pathogens. Food and water were available *ad libitum*. All animals were kept in individual cages. The housing and experimental protocols followed the guidelines of the Ministry of Education, Culture, Sports, Science, and Technology (MEXT) of Japan, and were in accordance with the Guide for the Care and Use of Laboratory Animals prepared by Okayama University (Okayama, Japan), by Tokyo Medical and Dental University (Tokyo, Japan), and by National Institute for Physiological Sciences (Okazaki, Japan). All efforts were made to minimize animal suffering and reduce the number of animals used in this study.

Ⅱ.2 | Experimental Procedures

Ⅱ.2.1 Tissue Processing

Hypothalamic sections and posterior pituitaries were obtained from four macaque monkeys (2 females and 2 males) as described previously [46]. Briefly, macaques were deeply anaesthetized with an overdose of sodium pentobarbital (~100 mg/kg body weight), and transcardially perfused with physiological saline followed by 4% paraformaldehyde (PFA) in 0.1 M phosphate buffer (PB, pH 7.4). After perfusion, brains and pituitaries were immediately removed and immersed in the same fixative for ~16 hours at 4 °C. Coronal 30-μm-thick sections of the hypothalamus were prepared with a Linear-Slicer (PRO10, Dosaka EM, Kyoto, Japan). Preparations were rinsed with PB and then immersed in antifreeze solution (30% glycerol, 30% ethylene glycol, 0.36% NaCl, and 0.05% NaN_3 in 40 mM PB) for storage at –25 °C until use. All the initial fixation was done 4–6 years before the present set of experiments. For Western blot analysis, three female macaques were sacrificed by blood loss under deep pentobarbital anesthesia (see above). Posterior pituitaries were quickly removed, frozen immediately in powdered dry ice, and stored at –80 °C until use.

Ⅱ.2.2 Immunofluorescence

The long-term stored, formaldehyde-fixed sections were rinsed with phosphate-buffered saline (PBS) containing 0.3% Triton X-100 (Sigma-Aldrich, St. Louis, MO, USA)

(PBST) five times for 10 minutes each. After blocking nonspecific binding with 1% normal goat serum and 1% BSA in PBST for 30 minutes at room temperature, the sections were incubated with mouse monoclonal anti-AVP-NPII antibody (PS41; 1:1,000 dilution) and with rabbit antiserum directed against copeptin (1:10,000 dilution) or with rabbit antiserum directed against CRF (1:20,000 dilution) for 4–5 days at 4 °C. The mouse monoclonal NPII antibody has previously shown to be specific for AVP neurons in rodents [31, 32] and macaque monkeys [46]. The copeptin$_{7–14}$ (ATQLDGPA) fragment, used as an antigen to produce the copeptin antiserum, is well conserved in mammals. It is identical in rats [29], mice [30], macaque monkeys [46], and humans [29]. The copeptin antiserum has also been characterized previously by immunohistochemistry [47], Western blot [28] and dot blot [47] analyses. The rabbit polyclonal antiserum against rat/human CRF (PBL rC70), which was kindly donated by Wylie Vale, has been characterized previously [33, 46, 47]. It was directed against the rat form of CRF, which is identical to the human form, and has also been characterized in non-human primates [34, 46]. Alexa Fluor 546-linked goat anti-mouse IgG (Molecular Probes, Eugene, OR, USA) and Alexa Fluor 488-linked goat anti-rabbit IgG (Molecular Probes) were used for detection at 1:1,000 dilution. Immunofluorescence studies were repeated independently at least three times using different macaques and always produced similar results. Immunostained sections were viewed by confocal laser scanning microscopy (FluoView 1000, Olympus, Tokyo, Japan). The information for antibodies used in this study is shown in Table 2.1.

Ⅱ.2.3 Post-Embedding Immunoelectron Microscopy

The long-term stored, formaldehyde-fixed sections were rinsed with PBS five times for 10 minutes each, and re-fixed in 4% PFA + 0.1% glutaraldehyde in 0.1 M PB for 4–6 hours at 4 °C. Sections were then rinsed with 0.1 M PB three times for 5 minutes each, and were dehydrated through increasing concentrations of methanol, flat-embedded in LR Gold resin (Electron Microscopy Sciences, Hatfield, PA, USA) by gently pressing against the bottom of the flat-bottom-capsule with a pre-prepared resin block, and polymerized under UV lamps at −25 °C for 24 hours. Ultrathin sections (70 nm in thickness) were collected on nickel grids coated with (or without for triple labeling) a collodion film, rinsed with PBS several times, then incubated with 2% normal goat serum and 2% BSA in 50 mM Tris(hydroxymethyl)-aminomethane-buffered saline (TBS; pH 8.2) for 20 minutes to block non-specific binding. The sections were then incubated with the mouse monoclonal antibody against NPII (1:200 dilution), with the rabbit polyclonal antisera against CRF (1:5,000 dilution), copeptin (1:100 dilution), L-glutamate (1:10

dilution, Abcam, Cambridge, UK), and/or with the guinea pig polyclonal antibody against VGLUT2 (1:20 dilution, Synaptic Systems, Göttingen, Germany) for 1 hour at room temperature. After incubation with the primary antibodies, the sections were washed with PBS, then incubated with a goat antibody against rabbit IgG conjugated to 5-nm or 10-nm gold particles (1:50 dilution, BBI Solutions, Cardiff, UK) and a goat antibody against mouse IgG conjugated to 15-nm gold particles (1:50 dilution, BBI Solutions) and/or a goat antibody against guinea pig IgG conjugated to 5-nm gold particles (1:50 dilution, Nanoprobes, Yaphank, NY, USA) for 1 hour at room temperature. The Abcam antibody to glutamate was raised in rabbit against L-glutamate conjugated to glutaraldehyde as the immunogen. The manufacturer's information shows no measurable cross-reactivity detected against glutamate in peptides or proteins but modest cross-reactivity against d-glutamate. The specificity of this antibody was confirmed by immunostaining in the rat retina [55]. To intensify the detectability of the immunoreaction for CRF in the cell body, a streptavidin-biotin intensification kit (Nichirei, Tokyo, Japan) was used. Tissues were first incubated with the biotinylated goat anti-rabbit IgG antibody for 10 minutes at room temperature, followed by incubation in avidin-biotin-horseradish peroxidase (HRP) complex solution for 5 minutes at room temperature. The sections were then washed with PBS, incubated with the goat antibody against HRP conjugated to 6-nm gold particles (1:50 dilution, Jackson ImmunoResearch Laboratory, West Grove, PA, USA) for 1 hour at room temperature.

Triple immunoelectron microscopy with antibodies against CRF, NPII, and glutamate was performed by using the front and back of ultrathin sections mounted on nickel grids without a supporting film. First, immunocytochemistry with a pair of primary antibodies (CRF and NPII) was performed on one side of the section and detected using 15-nm (mouse) and 10-nm (rabbit) colloidal gold particles (BBI Solutions), respectively. Next, immunocytochemistry with the other primary rabbit antibody (against glutamate) was performed on the other side of the section and detected by use of 5-nm colloidal gold particles (BBI Solutions). Immunoelectron microscopy studies were repeated independently at least three times using different macaques and always produced similar results.

Finally, the sections were contrasted with uranyl acetate and lead citrate and viewed using an H-7650 (Hitachi, Tokyo, Japan) or JEM-1010 (JEOL, Tokyo, Japan) electron microscope operated at 80 kV. The information for antibodies used in this study is shown in Table 2.1.

Ⅱ.2.4 Western Blotting

The lysates derived from posterior pituitaries were boiled in 10 μL sample buffer containing 62.5 mM trishydroxymethyl-aminomethane-HCl (Tris-HCl; pH. 6.8), 2% SDS, 25% glycerol, 10% 2-mercaptoethanol, and a small amount of bromophenol blue. These samples were run on a 4–20% SDS-PAGE and electroblotted onto a polyvinylidene difluoride (PVDF) membrane (Bio-Rad Laboratories, Hercules, CA, USA) from the gel by a semidry blotting apparatus (Bio-Rad Laboratories). The blotted membranes were blocked with PVDF Blocking Reagent for Can Get Signal (TOYOBO, Tokyo, Japan) for 30 minutes at room temperature and incubated overnight at 4 °C with anti-AVP-NPII mouse monoclonal antibody (PS41; 1:1,000 dilution) or anti-VGLUT2 guinea pig polyclonal antibody (1:10,000 dilution) in Can Get Signal Solution 1 (TOYOBO). The blotted membranes were rinsed three times with 0.05% Tween 20 in Tris-HCl-buffered saline (TBST) and incubated with horseradish peroxidase-conjugated goat polyclonal antibody against mouse IgG (Bio-Rad Laboratories) or guinea pig IgG (Bioss Inc., Woburn, MA, USA) 1:10,000 dilution in Can Get Signal Solution 2 (TOYOBO) for 1 hour at room temperature. After washing for three times with TBST, blots were visualized by Immun-Star WesternC Chemiluminescence Kit (Bio-Rad Laboratories). The information for antibodies used in this study is shown in Table 2.1. Western blotting analyses were repeated independently at least three times using different macaques and always produced similar results.

Ⅱ.3 | Statistical Analysis

All data values were expressed as mean ± standard error of the mean (SEM) and were analyzed using Statcel4 software. Statistical significance was determined as $p < 0.05$ using one-way analysis of variance (ANOVA). When significant difference was found by ANOVA, the *post hoc* Tukey–Kramer test was performed. All the various analyses in this study were conducted “blind”. All electron micrographs were coded and evaluated without the knowledge of the tissue, and the code was not broken until the analysis was complete.

Results

Antibody Characterization and the Expression of VGLUT2 at the Protein Level in the Posterior Pituitary

Full details of all the antibodies used in this study are shown in Table 2.1. The specificity for the VGLUT2 and NPII antibodies in Japanese macaque monkeys was first validated by Western blot analysis. Western blot analysis demonstrated the specificity for the guinea pig polyclonal antibody against VGLUT2 and the expression of VGLUT2 at the protein level in the posterior pituitary; a single strong immunoreactive band was detected at the expected molecular weight of ~56 kDa [56] (Figure 2.1). The mouse monoclonal antibody against AVP-neurophysin II (NPII) also detected a single major band at the expected molecular weight of ~12 kDa on the blots of posterior pituitary [46, 47] (Figure 2.1).

Anatomy of AVP-Producing Neurons in the Macaque Hypothalamus

Immunostaining for NPII was performed to study the localization of AVP neurons in the hypothalamus of Japanese macaque monkeys. Numerous magnocellular (large-sized) AVP neurons were observed in the PVN (Figure 2.2A) and SON (Figure 2.2B). Parvocellular (small-sized) AVP neurons were also observed in the PVN (Figure 2.2C). The median eminence can be divided into an internal and an external layer. The internal layer is the zone through which the axons of magnocellular neurons densely project into the posterior pituitary (Figure 2.2D) [2, 3, 38]. The external layer of the median eminence is where the axons of many parvocellular neurosecretory neurons, including parvocellular AVP/CRF neurons of the PVN, end on hypothalamo-hypophysial portal vessels and release anterior pituitary-hormone-regulating hormones (Figure 2.2D) [2, 3, 38].

In this study, immunoelectron microscopic characterization of AVP-producing neurons was performed in macaque hypothalamo-pituitary axis tissues fixed with 4% formaldehyde and stored at –25 °C for several years. It was found that both ultrastructure and immunoreactivity are sufficiently preserved in macaque brain tissues stored long-term, initially for light microscopy. Immunoelectron microscopy of the posterior pituitary showed many AVP dcv containing both NPII (PS41)- and copeptin (CP8)-immunoreactivity (Figure 2.3A, B). In other neighboring endings, no NPII- or copeptin-immunoreactivity was detectable (Figure 2.3C). In the median eminence, many dcv showing PS41/CP8 double-immunoreactivity were observed in both the internal and external layers (Figure 2.4). However, the AVP dcv in the internal layer (magnocellular)

of the median eminence (Figure 2.4B) were larger than those in the external layer (parvocellular) of the median eminence (Figure 2.4D).

Size Characterization of Dcv

Approximately 200 dcv in the neurosecretory axons in the posterior pituitary (magnocellular), the internal layer of the median eminence (magnocellular), and the external layer of the median eminence (parvocellular) were selected and their major axis diameters were measured. The average of major axis was 196 ± 2 nm in the posterior pituitary, 197 ± 2 nm in the internal layer of the median eminence, but significantly smaller (93 ± 1 nm) in the external layer of the median eminence (Figure 2.5; Table 2.2).

Next, the diameter of dcv in the perikarya of randomly selected SON and PVN AVP neurosecretory neurons was measured (at ×5,000 magnification; Table 2.3). In the SON (7 cell bodies), the average diameter of dcv contained in the cell body was 204 ± 12 nm (11 vesicles), confirming that, as expected, all AVP neurons in the SON are magnocellular (Figure 2.6; Table 2.3). The 18 AVP neurons in the PVN selected for analysis formed two distinct groups: those with larger dcv (180 ± 19 nm; 11 vesicles in Figure 2.7A, B) identified as magnocellular; and those with smaller dcv (102 ± 10 nm; 14 vesicles in Figure 2.7C, D) identified as parvocellular neurons.

A Subpopulation of Parvocellular AVP Neurons in the PVN Co-Expresses CRF

In the PVN, of the 18 AVP neuronal cell bodies analyzed, 6 were identified as magnocellular on the basis of vesicle size; none of these showed any CRF-immunoreactivity. Of the 12 PVN perikarya identified as parvocellular on the basis of vesicle size, a subpopulation (especially in the parvocellular part of the PVN) co-expressed CRF (Figure 2.8) and such neurons were more intermingled with magnocellular neurons in the macaque monkey than in rodent PVN as reported previously [34, 36, 46]. The terminal regions of parvocellular AVP/CRF neurons in the external layer of the median eminence were next analyzed (Figure 2.9). In these cells, the major axis diameter of the sparse dcv was 106 ± 3 nm (16 vesicles) (Figure 2.10) for the vesicles in the CRF-immunoreactive terminals, comparable to the 113 ± 9 nm (12 vesicles) in the cell body (Figure 2.11). In two putative parvocellular neurons (#24 and #25), the mean major axis of the dcv appeared slightly larger which might relate to the maturity of the vesicles (Table 2.3) [57].

Both Magno- and Parvocellular AVP Neurons Are Glutamatergic

Immunoelectron microscopy for L-glutamate was performed in the posterior pituitary in order to determine its occurrence in the terminal regions of magnocellular AVP neurons. The immunoreactivity for glutamate was associated primarily with the clusters of small electron-lucent vesicles in the axonal endings of AVP neurons of posterior pituitary (Figure 2.12A, B). In contrast, NPII-immunoreactivity was associated with dcv (Figure 2.12A, B). Next, the terminal regions of parvocellular axons in the median eminence were examined. Triple staining for CRF/NPII/glutamate (Figure 2.12C, D) showed that, as in the posterior pituitary, glutamate-immunoreactivity was associated with the clusters of electron-lucent microvesicles in the parvocellular endings which contained AVP/CRF-positive dcv (Figure 2.12C, D) and in other similar endings of the terminals of other parvocellular neurosecretory neurons. Due to the mild formaldehyde fixation, the membrane of single microvesicles could not be clearly distinguished. However, a comparison with glutaraldehyde-fixed material leaves no doubt that these are clusters of microvesicles. Similar results were obtained by immunoelectron microscopy for VGLUT2 in both the posterior pituitary and the external layer of the median eminence (Figure 2.13). Very few gold particles were associated with other intra-varicosity organelles, such as the mitochondria, and background labelling over glial and endothelial elements was also extremely low. Immunoelectron microscopy studies were repeated independently at least three times using different monkeys and always produced similar results.

Discussion

It is often assumed that glutaraldehyde, a cross-linking fixative, is essential for the preservation of fine ultrastructure [53, 54] and that formaldehyde-only fixed tissues are therefore inappropriate for electron microscopic analyses. However, the use of glutaraldehyde often results in a reduction of immunoreactivity and, for this reason, formaldehyde-fixed tissues without glutaraldehyde are used in most cases for immunohistochemical analysis at the light microscopic level [53, 54]. The current study demonstrates that, in the macaque brain, interpretable ultrastructure and adequate ultrastructural immunoreactivity are both preserved in brain tissue even after long-term storage at –25 °C for conventional light microscopy, provided that the fixed tissues are post-fixed with 0.1% glutaraldehyde after the long-term storage. Thus, formalin-fixed macaque brains stored for a long period, at least up to six-years in this study, can be used for immunoelectron microscopic analysis, suggesting that not only macaque brain, but also postmortem formalin-fixed human brain tissue could be amenable to immunoelectron microscopic analysis. It is also possible that it could be preserved over decades in antifreeze solution. Furthermore, the ultrastructure of tissues from rare animals such as endangered species might be studied in this way even if they had been prepared for light microscopic immunohistochemistry and stored at –25 °C in antifreeze solution.

The methodology used in this study has some obvious advantages in the ultrastructural analysis of the nervous system, in which tissue specimens are necessarily small, particularly where the brain is large, as in macaque monkeys and humans. After confirmation of the specificity of antibodies at the light microscopic level, post-embedding immunoelectron microscopic analysis can readily be performed on adjacent sections. Furthermore, because identification of brain nuclei and/or cells is easier at the light microscopic level, they can then be precisely targeted for post-embedding immunoelectron microscopy.

The size of dcv contained in the terminals of AVP neurons was quantified and compared among the posterior pituitary and internal/external layers of the median eminence. This showed, also for the macaque, the expected significant difference in size of the dcv (Figure 2.14). It is known that the posterior pituitary and the internal layer of the median eminence contain the axons of magnocellular AVP neurons of the PVN and SON, whereas the external layer of the median eminence is the terminal region of parvocellular AVP neurons of the PVN [2, 3, 38] and other parvocellular neurons influence the anterior pituitary. In the dcv of the internal layer of the median eminence through which the magnocellular axons pass *en route* to the posterior pituitary, the AVP

precursor should be processed sufficiently to reveal both prominent NPII- and copeptin-immunoreactivity in almost all of the axons [36, 38, 46]. In the macaque hypothalamus, quantifying only the size of the dcv in the cell body or its axon enables identification of the magnocellular or parvocellular neurons. Finally, it was confirmed at the electron microscopic level that certain axonal endings in the external layer of the median eminence of macaques are derived from parvocellular AVP neurons of the PVN.

It has been reported that rodent AVP neurons use glutamate as a neurotransmitter [50, 51, 58, 59]. In this study, the detectability and thus the expression of glutamate and VGLUT2 in the macaque posterior pituitary were examined. Western blotting first demonstrated that VGLUT2 was expressed in the macaque posterior pituitary, suggesting that magnocellular AVP (and also oxytocin) neurons use glutamate as a neurotransmitter in Japanese macaque monkeys. Immunoelectron microscopic analysis revealed that the AVP/CRF-immunoreactivity was restricted to the dcv, but the VGLUT2-immunoreactivity was associated with the smaller, electron-lucent microvesicles (Figure 2.14). Similarly, immunoreactivity for glutamate itself was essentially restricted to regions containing clusters of microvesicles in the axonal endings of AVP neurons in both the posterior pituitary and external layer of the median eminence (Figure 2.14). Because the antibody for glutamate, an amino acid, is raised against the cross-linking site of glutaraldehyde as the antigen, it is thought to be essential that glutaraldehyde is included in the fixative prior to glutamate immunocytochemistry [50, 51, 55]. Although glutaraldehyde was not included in the primary perfusion fixative, post-fixation of the formaldehyde-fixed tissue with glutaraldehyde permitted detection of glutamate by immunoelectron microscopy even after prolonged storage. Therefore, the subcellular localization of amino acids appears, surprisingly, to be preserved for a long period even after conventional formaldehyde fixation. These results suggest that the immunoelectron microscopic detection of amino acids including glutamate and GABA would also be possible in conventional formaldehyde-fixed and stored human brain tissue.

These results in macaque tissue show that glutamate as an excitatory neurotransmitter is in microvesicles both in magno- and parvocellular AVP neurons. Although the localization of glutamate receptors has been reported in the neural lobe, median eminence and anterior pituitary, a clear role for glutamate secretion at these sites remains unknown [60, 61]. Salt loading has been shown to produce robust increases in the *VGLUT2* mRNA of AVP neuron perikarya and in VGLUT2-immunoreactivity in the rat posterior pituitary [62], suggesting that an osmotic challenge could produce an increase in glutamate release in the primate magnocellular AVP system (Figure 2.14). Similarly, a role in the anterior pituitary of glutamate released from parvocellular

AVP/CRF neurons into the hypothalamo-hypophysial portal veins remains unclear. Functional implications for glutamate release at the terminals of both magno- and parvocellular AVP neurons remain to be explored.

Conclusions

This study reports the immunoelectron microscopic characterization of AVP-producing neurons in primate hypothalamo-pituitary systems by the use of formaldehyde-fixed tissues stored at –25 °C for up to six years. The size difference in dcv between magno- and parvocellular AVP neurons in Japanese macaque monkeys was determined (Figure 2.14). Furthermore, despite the prolonged fixation and storage, the size of the magno- and parvocellular dcv was virtually identical to that observed in freshly fixed and embedded tissue [3, 28, 63-66]. Immunoelectron microscopy also demonstrated that both magno- and parvocellular AVP neurons are glutamatergic in primates (Figure 2.14). These results show, for the macaque brain, that interpretable neuronal ultrastructure and sufficient immunoreactivity for several relevant proteins are preserved even after a long-term storage of tissues fixed in formaldehyde for light microscopy. They indicate that this methodology could be applied to human post-mortem brain and, therefore, be very useful in translational research.

List of Tables and Figures

Chapter 2 – Tables

Chapter 2 – Figures

Table 2.1 Primary antibodies used in this study

Antigen	Description	Source, Host Species, Cat#, or Code#	Working Dilution	Reference#	RRID
Copeptin	Synthetic peptide mapping at the amino acids 7–14 of human/mouse copeptin	Generated by our laboratory, rabbit polyclonal, CP8	1:10,000 (IF) 1:100 (EM)	[28, 46, 47]	AB_2722604
CRF	Human/rat CRF coupled to human α-globulins *via* bis-diazotized benzidine	Donated by Dr. W. Vale, rabbit polyclonal, PBL rC70	1:20,000 (IF) 1:5,000 (EM)	[33, 34, 46]	AB_2314234
NPII	Soluble proteins extracted from the posterior pituitary of the rat	ATCC, mouse monoclonal, PS41, CRL-1799	1:1,000 (IF) 1:200 (EM) 1:1,000 (WB)	[31, 32, 45, 46]	AB_2313960
VGLUT2	Recombinant protein corresponding to amino acids 510–582 of the rat VGLUT2	Synaptic Systems, guinea pig polyclonal, 135 404	1:20 (EM) 1:10,000 (WB)	[67, 68]	AB_887884
L-Glutamate	L-Glutamate conjugated to glutaraldehyde	Abcam, rabbit polyclonal, ab9440	1:10 (EM)	[55, 69]	AB_307256

Abbreviations: ATCC, American Type Culture Collection; Cat, catalogue; CRF, corticotropin-releasing factor; EM, immunoelectron microscopy; IF, immunofluorescence; NPII, arginine vasopressin-associated neurophysin II; RRID, research resource identifier; VGLUT2, vesicular glutamate transporter 2; WB, Western blotting; #, number.

Table 2.2 Identification of cell types (magno- or parvocellular neurons) based on the major axis of dense-cored neurosecretory vesicles

Region	Major Axis (nm)	Magno or Parvo	Number of Vesicles Examined	Identification
Posterior pituitary	196 ± 2	Magno	205	AVP
Internal ME	197 ± 2	Magno	237	AVP without CRF
External ME	93 ± 1 *	Parvo	212	CRF

AVP, arginine vasopressin; internal ME, internal layer of the median eminence; CRF, corticotropin-releasing factor; external ME, external layer of the median eminence. * $p < 0.05$, vs. posterior pituitary and internal layer of the median eminence. All data values are presented as mean ± standard error of the mean (SEM).

Table 2.3 Characterization of cell types (magno- or parvocellular neurons) based on the major axis of dense-cored neurosecretory vesicles

Cell Body	Major Axis (nm)	Magno or Parvo	Number of Vesicles Examined	SON or PVN	Identification
#1	187 ± 5 *	Magno	29	SON	AVP
#2	175 ± 6 *	Magno	35	SON	AVP
#3	189 ± 10 *	Magno	24	SON	AVP
#4	181 ± 5 *	Magno	26	SON	AVP
#5	171 ± 7 *	Magno	25	SON	AVP
#6	195 ± 6 *	Magno	30	SON	AVP
#7	205 ± 6 *	Magno	46	SON	AVP
#8	188 ± 5 *	Magno	49	PVN	AVP
#9	170 ± 5 *	Magno	20	PVN	AVP
#10	169 ± 8 *	Magno	22	PVN	AVP
#11	172 ± 4 *	Magno	24	PVN	AVP
#12	184 ± 5 *	Magno	25	PVN	AVP
#13	182 ± 5 *	Magno	21	PVN	AVP
#14	103 ± 5 †	Parvo	38	PVN	AVP
#15	98 ± 4 †	Parvo	42	PVN	CRF
#16	109 ± 4 †	Parvo	51	PVN	CRF
#17	93 ± 5 †	Parvo	24	PVN	CRF
#18	107 ± 5 †	Parvo	40	PVN	CRF
#19	103 ± 4 †	Parvo	35	PVN	CRF
#20	110 ± 7 †	Parvo	42	PVN	CRF
#21	108 ± 5 †	Parvo	77	PVN	CRF
#22	93 ± 4 †	Parvo	81	PVN	CRF
#23	95 ± 5 †	Parvo	30	PVN	CRF
#24	120 ± 6 *,†	(Parvo)	40	PVN	CRF
#25	113 ± 3 *,†	(Parvo)	89	PVN	CRF

AVP, arginine vasopressin; CRF, corticotropin-releasing factor; SON, supraoptic nucleus; PVN, paraventricular nucleus; #, number. * $p < 0.05$, vs. external layer of the median eminence; † $p < 0.05$, vs. posterior pituitary and internal layer of the median eminence. All data values are presented as mean ± standard error of the mean (SEM).

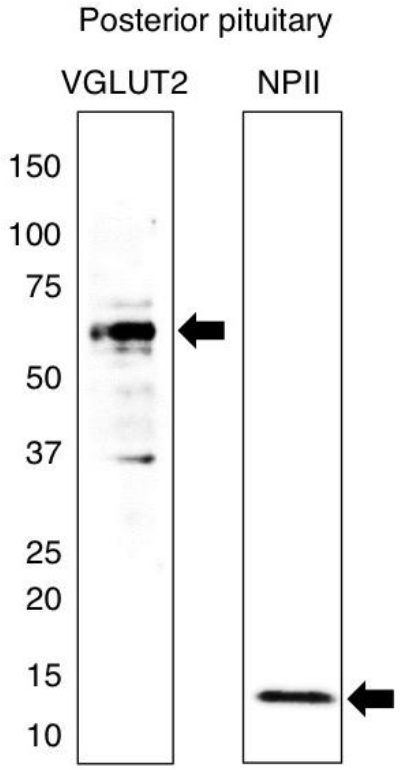

Figure 2.1 Western immunoblotting of vesicular glutamate transporter 2 (VGLUT2) and vasopressin-associated neurophysin (NPII). The number on the left indicates the molecular weight (kDa). Extracts of protein from the posterior pituitary of the Japanese macaque monkey were transferred onto polyvinylidene difluoride membranes and probed with the guinea pig polyclonal antiserum against VGLUT2 or with the mouse monoclonal antibody against NPII. The antisera recognized a single major band at the expected molecular weight of VGLUT2 (~56 kDa) or NPII (~12 kDa) on a Western blot of the macaque posterior pituitary.

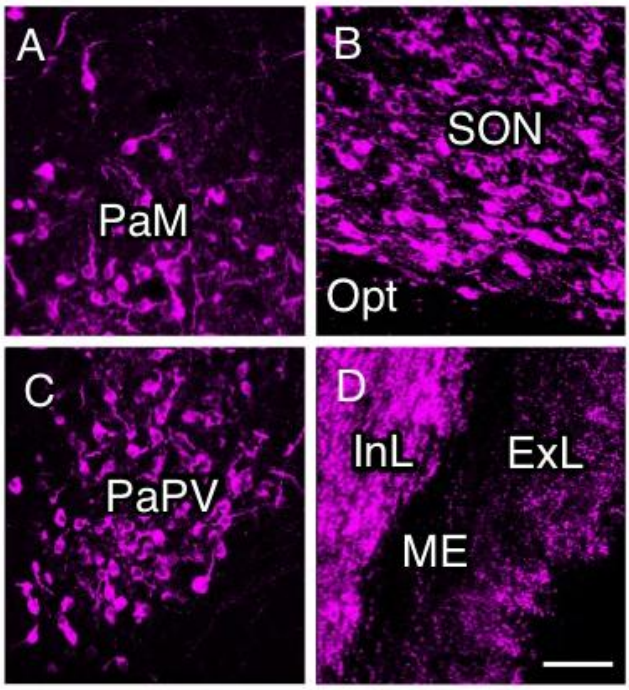

Figure 2.2 Immunofluorescence for vasopressin-associated neurophysin (NPII) in the macaque hypothalamus. NPII-immunoreactivity was observed in the paraventricular nucleus (PVN) of the hypothalamus; PaM, magnocellular part of the PVN (**A**); supraoptic nucleus (**B**); PaPV, parvocellular part of the PVN, ventral division (**C**); and median eminence (ME) (**D**). Opt, optic nerve; InL, internal layer of the ME; ExL, external layer of the ME. *Scale bar*, 100 μm.

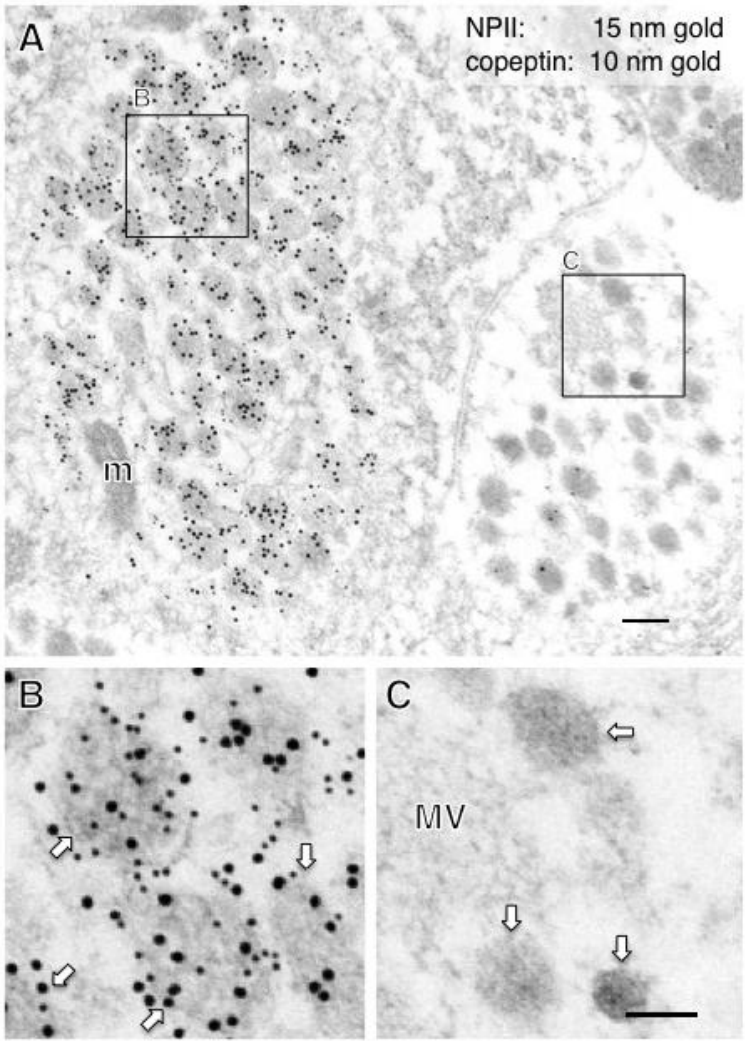

Figure 2.3 Double-label immunoelectron microscopy for vasopressin-associated neurophysin (NPII) and copeptin in the macaque posterior pituitary. Numerous neurosecretory vesicles located in some of the varicosities were doubly immunopositive for copeptin (10-nm gold particles) and NPII (15-nm gold particles). The outlined areas in (**A**) are enlarged in (**B**, **C**). In contrast, in other presumably oxytocin-containing varicosities, no NPII/copeptin-immunoreactivity was detected (**A**, **C**). *Scale bars*, 200 nm, and 100 nm in enlarged images. *Arrows* indicate dense-cored neurosecretory vesicles. m, mitochondrion; MV, clustered microvesicles.

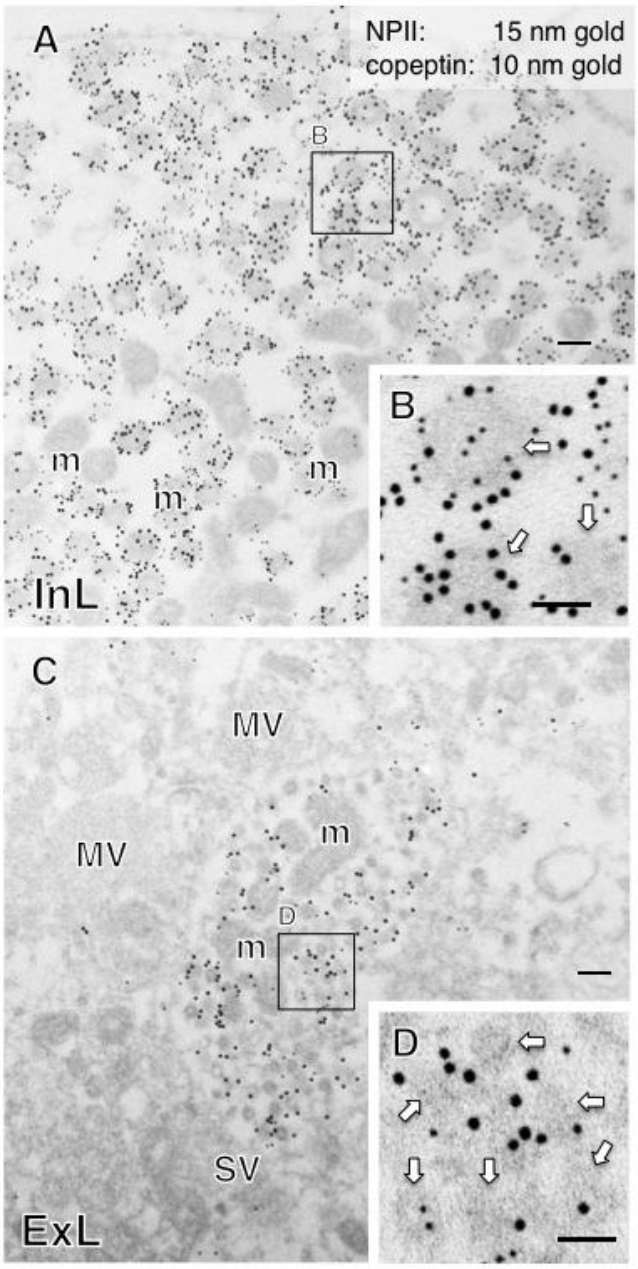

Figure 2.4 Double-label immunoelectron microscopy for vasopressin-associated neurophysin (NPII) and copeptin in the internal layer (InL; (**A**, **B**)) and external layer (ExL; (**C**, **D**)) of the macaque median eminence. Numerous dense-cored neurosecretory vesicles located in some of the varicosities were immunopositive for both copeptin (10-nm gold particles) and NPII (15-nm gold particles). The outlined area in (**A**) and (**C**) is enlarged in (**B**) and (**D**), respectively. *Scale bars*, 200 nm, and 100 nm in enlarged images. *Arrows* indicate dense-cored neurosecretory vesicles. m, mitochondrion; MV, clustered microvesicles.

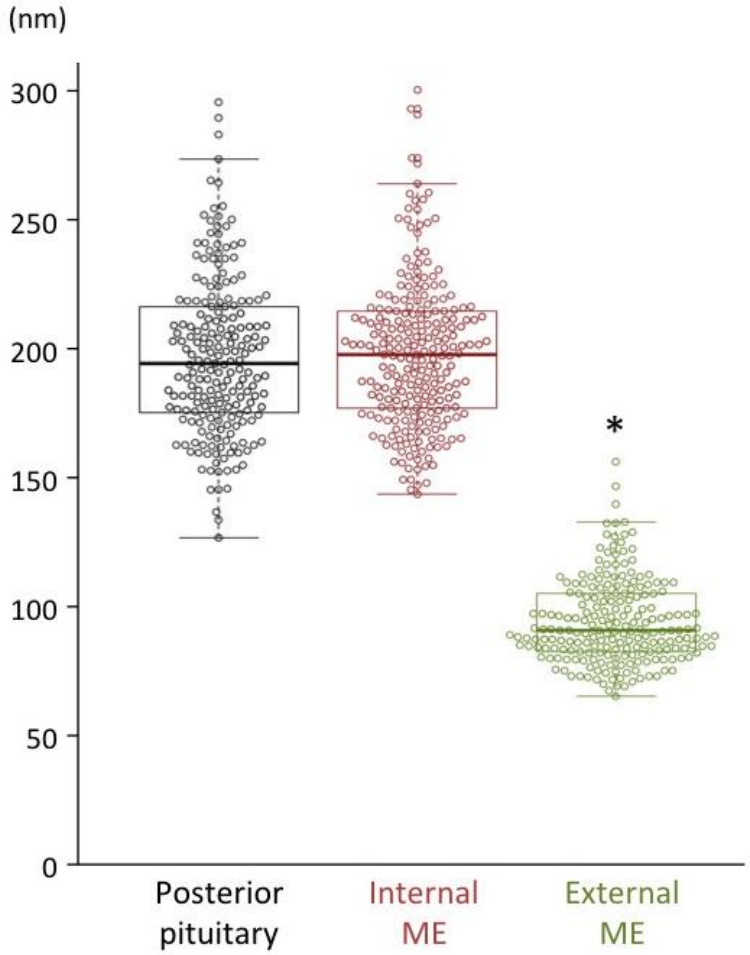

Figure 2.5 Bee-swarm and box plots displaying the major axis of dense-cored neurosecretory vesicles distributed in the posterior pituitary (black), internal layer of the median eminence (ME) (red), and external layer of the ME (green) in macaque monkeys. The major axis of dense-cored vesicles in the posterior pituitary and the internal layer of the ME (~200 nm) was significantly larger than that of the vesicles in the external layer of the ME (~100 nm). * $p < 0.05$, vs. posterior pituitary and internal layer of the ME.

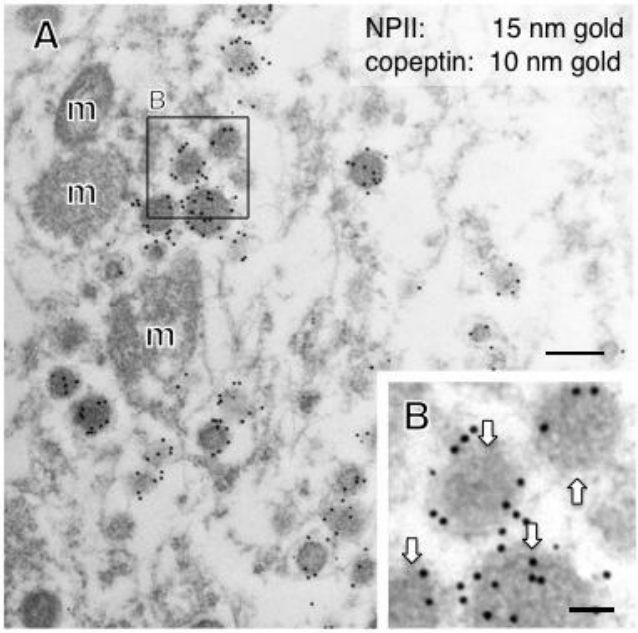

Figure 2.6 Double-label immunoelectron microscopy for vasopressin-associated neurophysin (NPII) and copeptin in the macaque supraoptic nucleus (SON). Many dense-cored neurosecretory vesicles located in the cell body were doubly immunopositive for copeptin (10-nm gold particles) and NPII (15-nm gold particles). The outlined area in (**A**) is enlarged in (**B**). *Scale bars*, 200 nm, and 100 nm in the enlarged image. *Arrows* indicate dense-cored neurosecretory vesicles. m, mitochondrion.

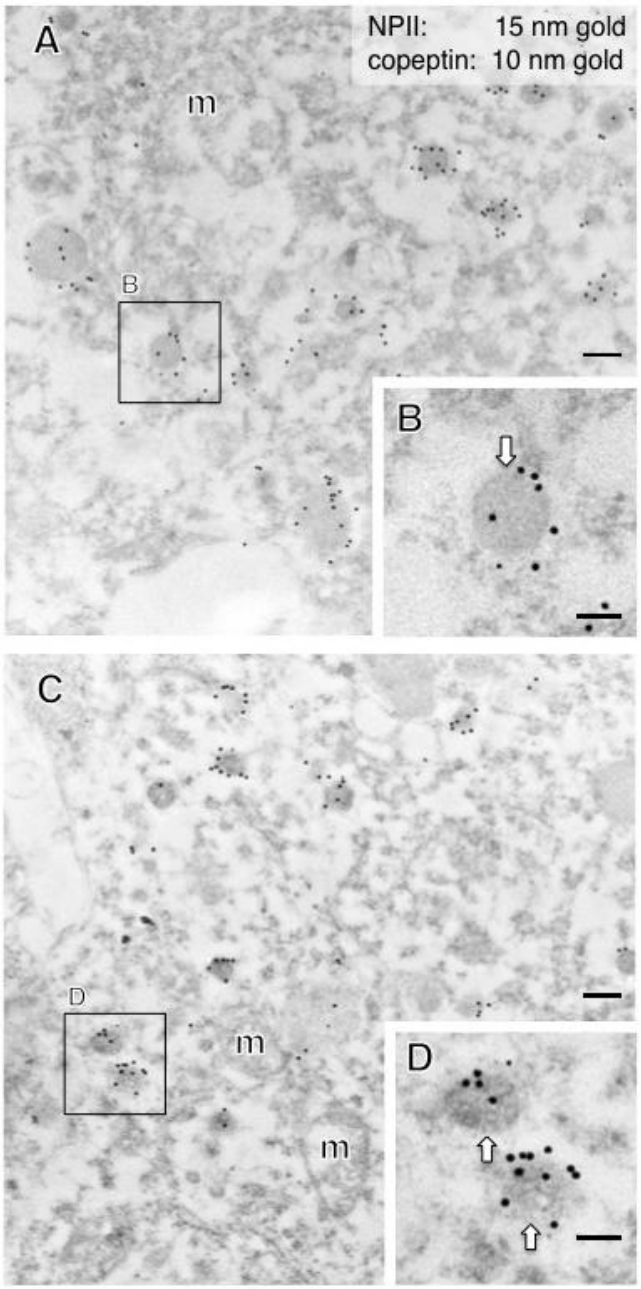

Figure 2.7 Double-label immunoelectron microscopy for vasopressin-associated neurophysin (NPII) and copeptin in the macaque paraventricular nucleus (PVN) of the hypothalamus. (**A**) In the cell body of a putative magnocellular vasopressin neuron, many dense-cored neurosecretory vesicles located in the cell body were doubly immunopositive for copeptin (10-nm gold particles) and NPII (15-nm gold particles). (**C**) Similar results are obtained in the cell body of a putative parvocellular vasopressin neuron. The size of dense-cored vesicles in (**A**, **B**) was larger than that of vesicles in (**C**, **D**). The outlined areas are enlarged. *Scale bars*, 200 nm, and 100 nm in enlarged images. *Arrows* indicate dense-cored neurosecretory vesicles. m, mitochondrion.

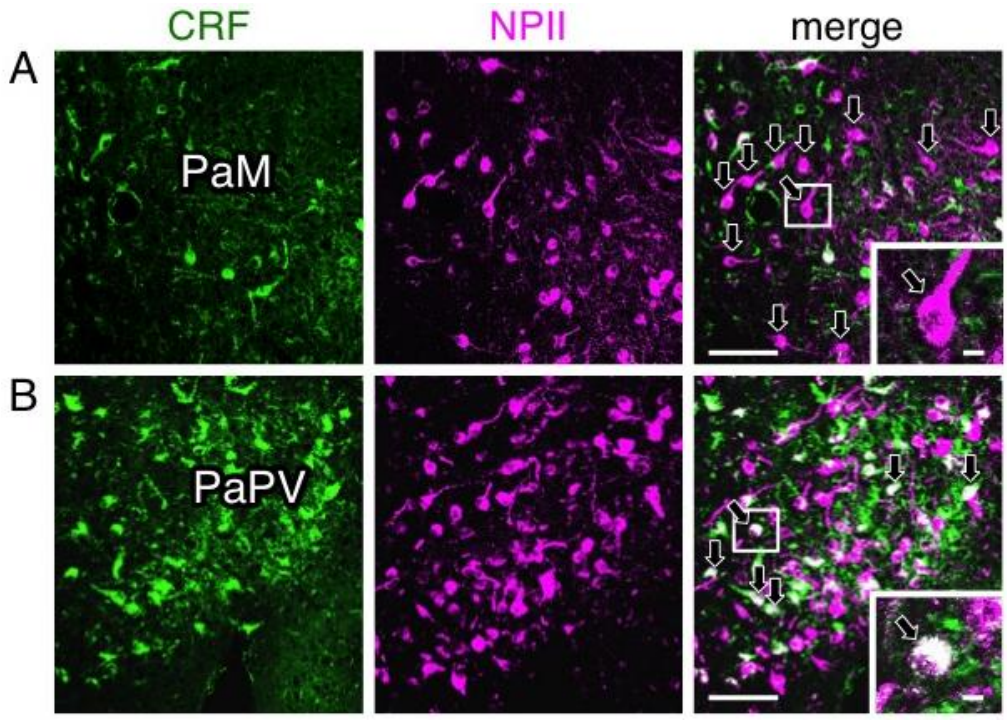

Figure 2.8 Double-label immunofluorescence for corticotropin-releasing factor (CRF) and vasopressin-associated neurophysin (NPII) in the paraventricular nucleus (PVN) of the macaque hypothalamus; PaM, magnocellular part of the PVN (**A**); PaPV, parvocellular part of the PVN, ventral division (**B**). Immunoreactivity against CRF (green) and NPII (magenta) is merged in each right-hand *panel* (overlap; white). The outlined areas in merged images are enlarged. *Arrows* in (**A**; merged) indicate perikarya single-immunopositive for NPII in the PaM. *Arrows* in (**B**; merged) indicate doubly immunopositive for CRF and NPII in the PaPV. *Scale bars*, 100 µm, and 10 µm in enlarged images.

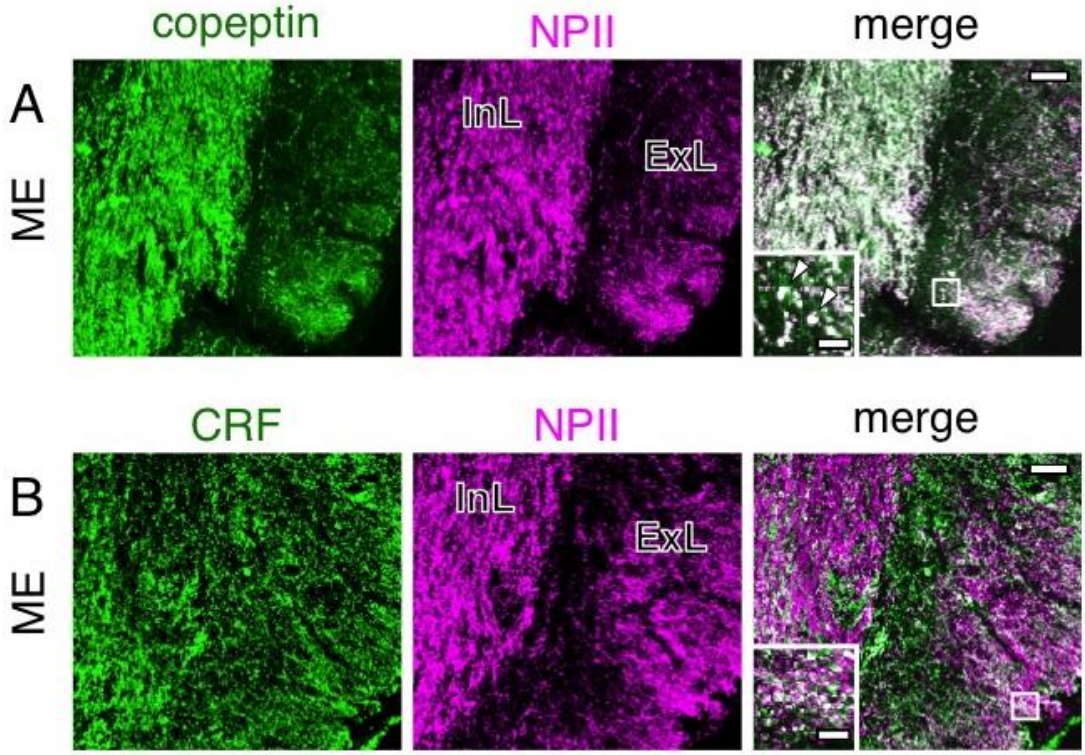

Figure 2.9 Double-label immunofluorescence for copeptin (**A**) or corticotropin-releasing factor (CRF) (**B**) and vasopressin-associated neurophysin (NPII) in the macaque median eminence (ME). Immunoreactivity against copeptin (**A**; green) or CRF (**B**; green) and NPII (magenta) is merged in each right-hand *panel* (overlap; white). The outlined areas in merged images are enlarged. *Arrowheads* in (**A**) indicate tissue doubly immunopositive for copeptin and NPII. *Scale bars*, 50 µm, and 10 µm in enlarged images. InL, internal layer of the ME; ExL, external layer of the ME.

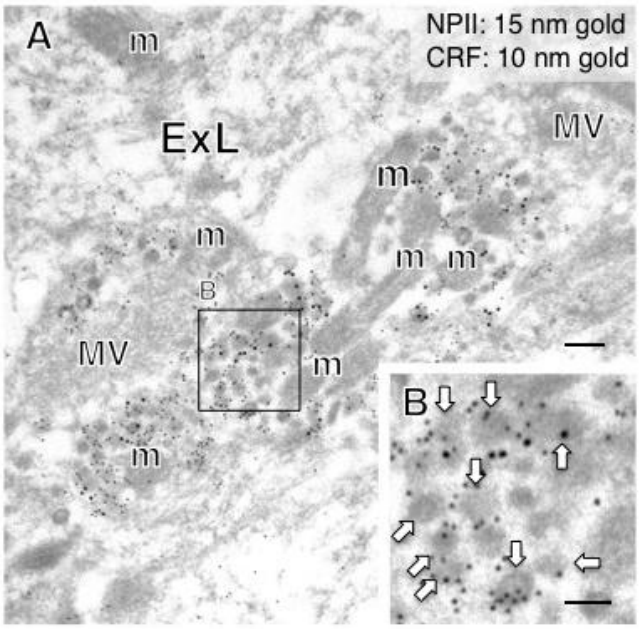

Figure 2.10 Double-label immunoelectron microscopy for vasopressin-associated neurophysin (NPII) and corticotropin-releasing factor (CRF) in the external layer (ExL) of the macaque median eminence. In some axonal varicosities, numerous dense-cored neurosecretory vesicles were doubly immunopositive for CRF (10-nm gold particles) and NPII (15-nm gold particles). The outlined area in (**A**) is enlarged in (**B**). *Scale bars*, 200 nm, and 100 nm in the enlarged image. *Arrows* indicate dense-cored neurosecretory vesicles. m, mitochondrion; MV, clustered microvesicles.

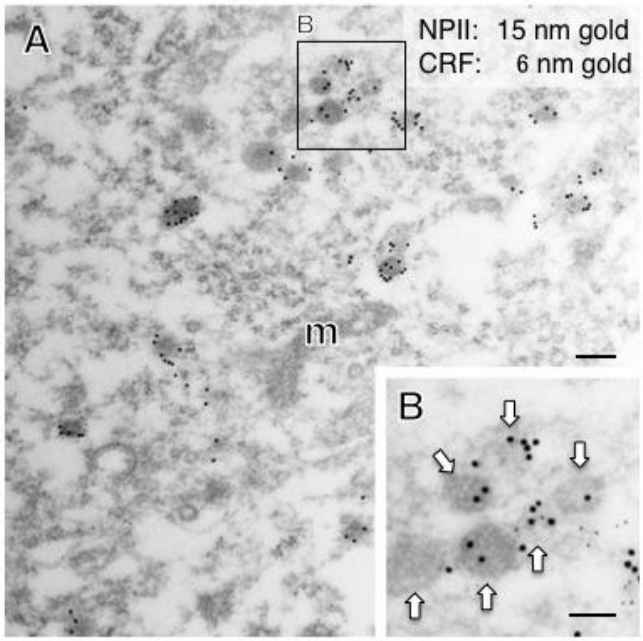

Figure 2.11 Double-label immunoelectron microscopy for vasopressin-associated neurophysin (NPII) and corticotropin-releasing factor (CRF) in the paraventricular nucleus (PVN) of the hypothalamus in a macaque monkey. (**A**) In the cell body of a possible parvocellular vasopressin neuron, many dense-cored neurosecretory vesicles located in the cell body were doubly immunopositive for CRF (6-nm gold particles) and NPII (15-nm gold particles). The outlined area in (**A**) is enlarged in (**B**). *Scale bars*, 200 nm, and 100 nm in the enlarged image. *Arrows* indicate dense-cored neurosecretory vesicles. m, mitochondrion.

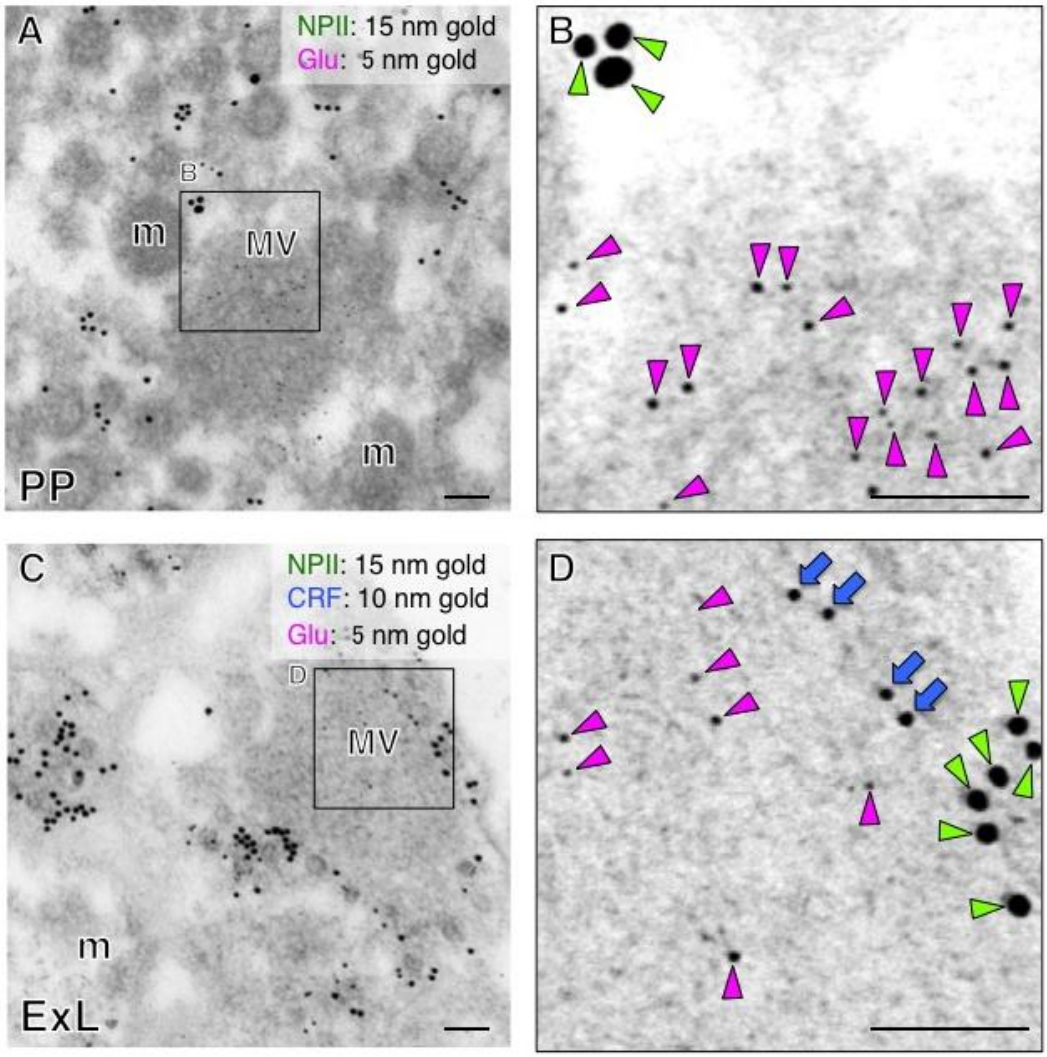

Figure 2.12 Immunoelectron microscopy for glutamate (Glu) in the posterior pituitary (PP) (**A**) and external layer of the median eminence (ExL) (**C**) in a macaque monkey. (**B**) Double-label immunoelectron microscopy for vasopressin-associated neurophysin (NPII) and Glu shows that Glu-immunoreactivity is associated with microvesicles in the macaque posterior pituitary. (**D**) Triple-label immunoelectron microscopy for NPII/corticotropin-releasing factor (CRF)/Glu indicates that Glu-immunoreactivity is associated with electron-lucent small vesicles in the axonal endings, in the NPII/CRF-double positive endings. The outlined areas are enlarged. *Scale bars*, 100 nm. *Green arrowheads* indicate NPII-immunoreactivity; *blue arrows* indicate CRF-immunoreactivity; *magenta arrowheads* indicate Glu-immunoreactivity. m, mitochondrion; MV, clustered microvesicles.

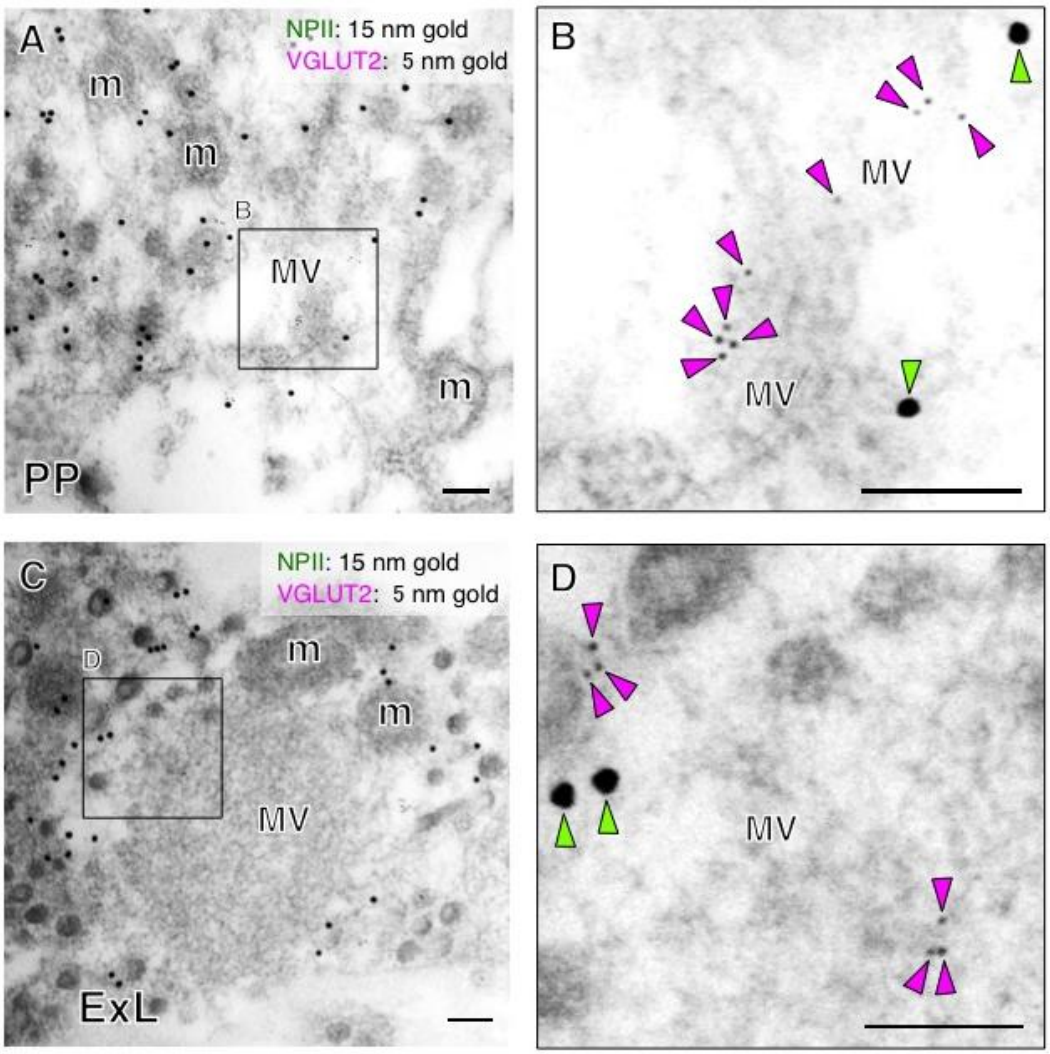

Figure 2.13 Immunoelectron microscopy for vesicular glutamate transporter 2 (VGLUT2) in the posterior pituitary (PP) (**A**) and external layer of the median eminence (ExL) (**C**) in a macaque monkey. (**B**) Double-label immunoelectron microscopy for vasopressin-associated neurophysin (NPII) and VGLUT2 shows that VGLUT2-immunoreactivity is associated with clustered microvesicles (MV) in the posterior pituitary. (**D**) Double-label immunoelectron microscopy for NPII/VGLUT2 indicates that VGLUT2-immunoreactivity is associated with the membrane of electron-lucent small vesicles in the vasopressin endings. The outlined areas are enlarged. *Scale bars*, 100 nm. *Green arrowheads* indicate NPII-immunoreactivity; *magenta arrowheads* indicate VGLUT2-immunoreactivity. m, mitochondrion; MV, clustered microvesicles.

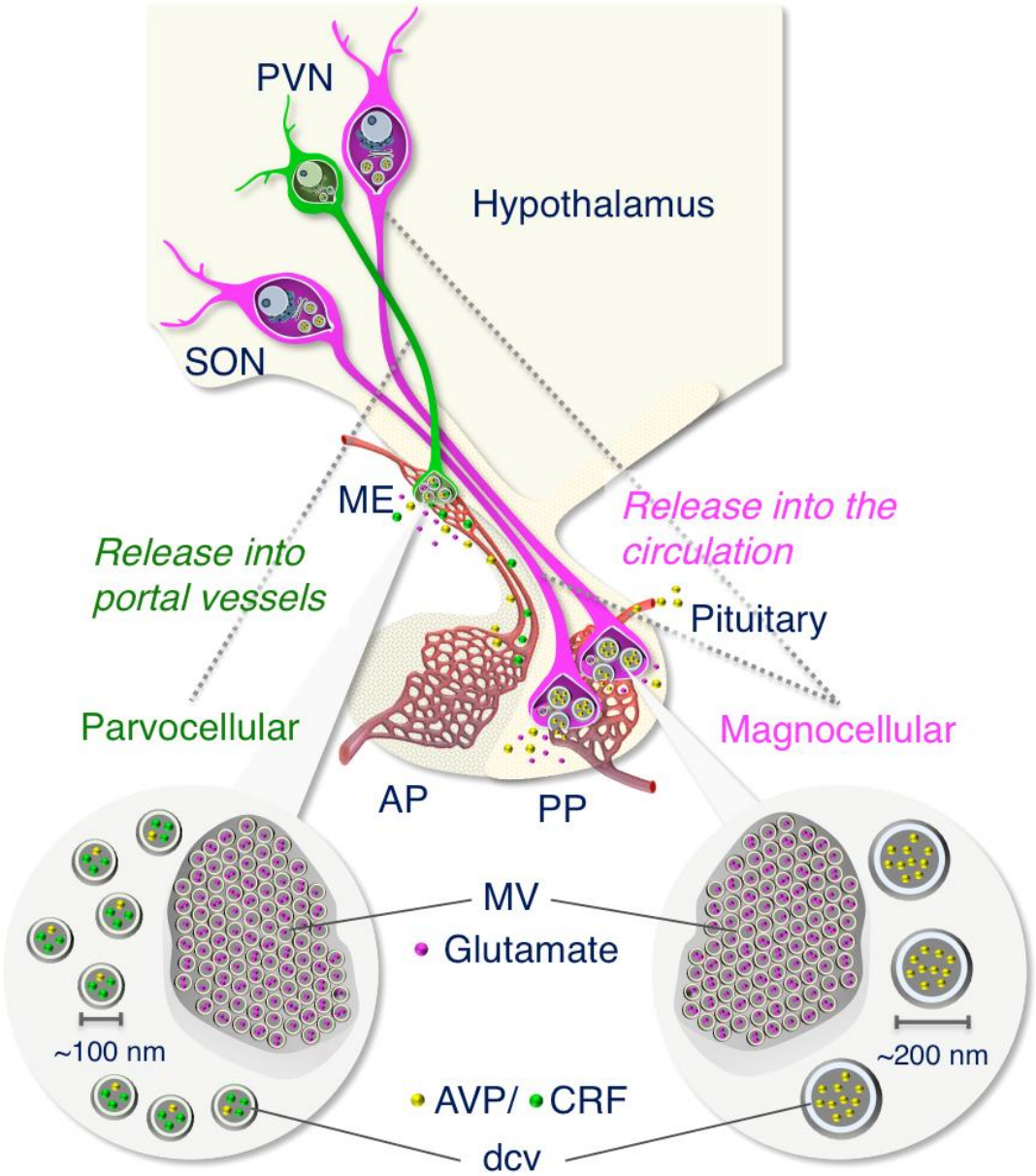

Figure 2.14 Working model showing that the size difference in dense-cored neurosecretory vesicles (dcv) between magnocellular (~200 nm) and parvocellular (~100 nm) vasopressin (AVP)- and/or corticotropin-releasing factor (CRF)-producing neurons in the hypothalamus of the Japanese macaque monkey. Both magno- and parvocellular AVP/CRF neurons are glutamatergic in primates. AP, anterior pituitary; ME, median eminence; MV, clustered microvesicles; PP, posterior pituitary; PVN, paraventricular nucleus; SON, supraoptic nucleus.

General Discussion

This dissertation provides novel insights into how the ultrastructural organization of arginine vasopressin (AVP) neurons supports their functional roles in the macaque neuroendocrine system.

In Chapter 1, the intracellular localization and functional significance of AVP and corticotropin-releasing factor (CRF) in the macaque neuroendocrine system were examined. In rodents, parvocellular AVP neurons co-localize CRF within the same dense-core vesicles, and co-release of their peptides synergistically enhances adrenocorticotropic hormone (ACTH) secretion. This co-localization pattern is closely associated with the synergistic stress-response mechanism mediated by coordinated AVP/CRF release; however, it remains uncharacterized in primates. To address this question, parvocellular AVP neurons in macaques were examined to determine whether this co-localization pattern occurs. First, reverse transcription (RT)-PCR confirmed expression of *AVP* and *CRF* mRNA in the paraventricular nucleus (PVN) of the hypothalamus. Next, fluorescence immunohistochemistry was used to examine whether AVP and CRF co-localize within the same neurons. As a result, among CRF-positive cells, AVP-immunoreactivity was observed in approximately 40% in the PVN and approximately 50% in the external layer of the median eminence (ME), demonstrating peptide co-expression at the cellular level. These findings indicate co-localization of AVP and CRF within the same cells; however, to assess the potential for coordinated release, verification of their co-localization within individual dense-core vesicles was required. Hence, to assess vesicular co-localization, AVP and CRF distribution within dense-core vesicles was examined by immunoelectron microscopy. In the external layer of the ME, individual dense-core vesicles exhibited immunoreactivity for both AVP and CRF,

demonstrating co-packaging within the same vesicles in the macaque (Figure GD.1). This ultrastructural feature provides the molecular basis for their synergistic release under stress, enhancing ACTH secretion *via* the hypophyseal portal system and amplifying activation of the hypothalamic–pituitary–adrenal (HPA) axis. Taken together, these findings suggest that macaques also possess a potent stress-response mechanism mediated by coordinated AVP/CRF release.

In Chapter 2, ultrastructural characterization of AVP neurons in the macaque was conducted to examine how their morphological characteristics relate to functional diversity. First, immunoelectron microscopy was used to analyze the morphology of dense-core vesicles in magnocellular and parvocellular AVP neurons, which have different functions. Guided by AVP and CRF immunolabeling, dense-core vesicle sizes were measured in the posterior pituitary (magnocellular), the internal layer of the ME (magnocellular), and the external layer of the ME (parvocellular). As a result, dense-core vesicle diameters were found to average approximately 200 nm in both the posterior pituitary and the internal layer of the ME; however, they were significantly smaller—approximately 100 nm—in the external layer of the ME (Figure GD.2). This difference in dense-core vesicle size is thought to represent a morphological feature reflecting the functional distinctions between magnocellular and parvocellular AVP neurons. Furthermore, in rodents, AVP neurons utilize glutamate as a neurotransmitter, and the co-release of AVP and glutamate may contribute to the diverse functional regulation of AVP neurons. However, it remains unclear whether primate AVP neurons employ a comparable dual-transmission system. Therefore, to verify whether macaque AVP neurons also possess a dual release system consisting of AVP released from dense-core vesicles and glutamate released from synaptic vesicles, their glutamatergic phenotype

was examined. Immunoelectron microscopy of the posterior pituitary and the external layer of the ME revealed immunoreactivity for glutamate and vesicular glutamate transporter 2 (VGLUT2) in AVP-positive nerve terminals. Additionally, unlike AVP and CRF, which localize to dense-core vesicles, glutamate and VGLUT2-immunoreactivity were confined to synaptic vesicles of approximately 50 nm in diameter. Thus, macaque AVP neurons are also glutamatergic, demonstrating the ultrastructural feature that AVP and glutamate are localized to distinct types of release vesicles (Figure GD.2). Macaque AVP neurons possess two types of release vesicles—dense-core vesicles (approximately 100–200 nm) storing AVP and synaptic vesicles (approximately 50 nm) storing glutamate—enabling diverse functional regulation through differential patterns of peptide hormone and neurotransmitter release.

In summary, this study clarified one aspect of the functional–morphological relationships of AVP in the macaque neuroendocrine system. The ultrastructural features of AVP neurons in the macaque neuroendocrine system—such as co-localization of AVP and CRF, differences in release-vesicle sizes, and localization of glutamate-related molecules—suggest a universal mechanism shared with rodents. These findings are expected to provide critical basic molecular data for elucidating the pathophysiology of human AVP-related disorders and for developing future therapeutic approaches.

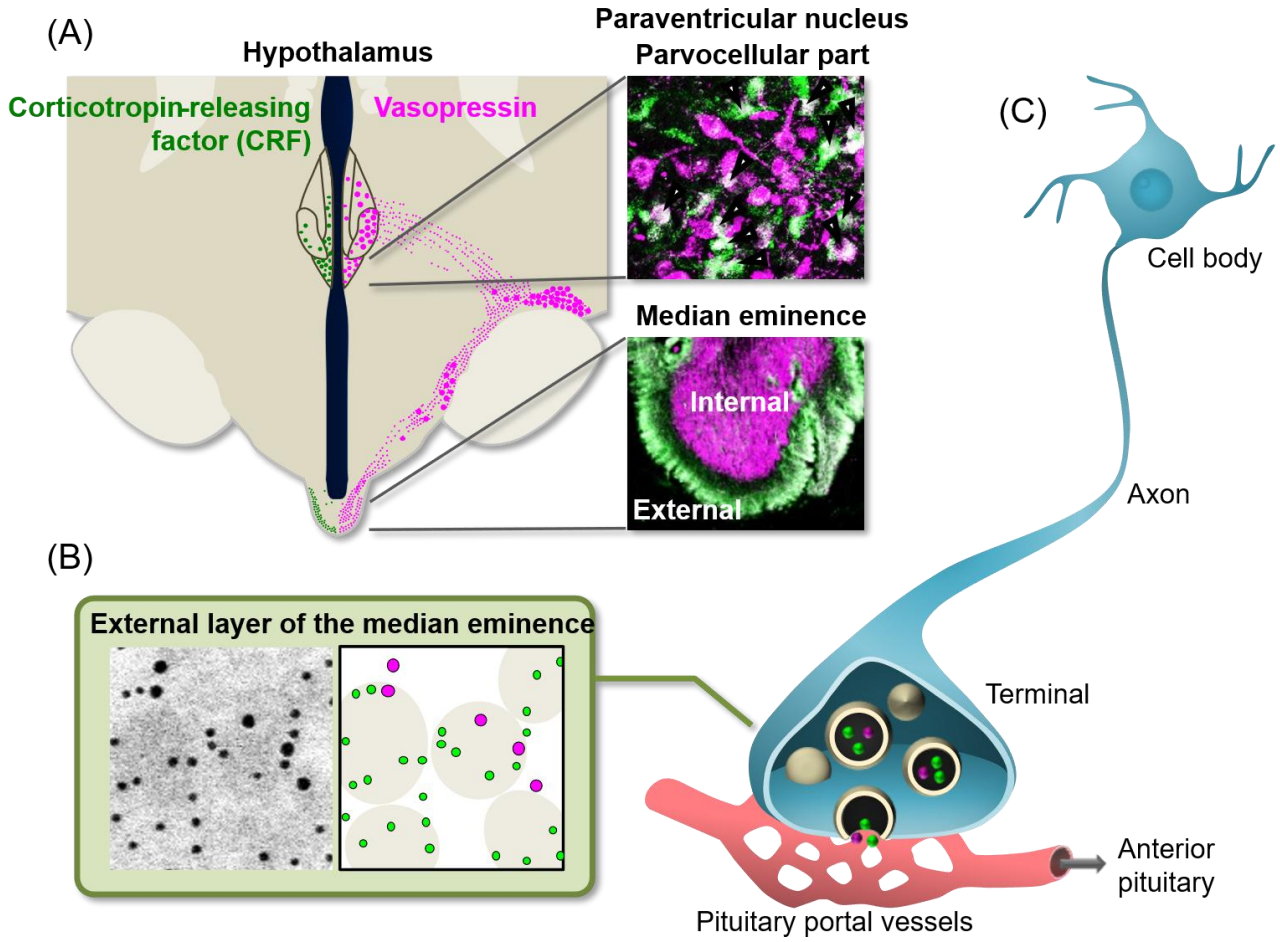

Figure GD.1 (**A**) Diagram of the distribution of vasopressin (AVP)- expressing neurons (magenta) and corticotropin-releasing factor (CRF)-expressing neurons (green) in the macaque hypothalamus. Double-label immunofluorescence in the paraventricular nucleus and median eminence (ME) shows AVP-immunoreactive neurons (magenta) and CRF-immunoreactive neurons (green). (**B**) Double-label immunoelectron microscopy for AVP and CRF in the external layer of the ME. Magenta circles indicate AVP-immunoreactivity; Green circles indicate CRF-immunoreactivity. (**C**) Schematic diagram of the parvocellular neuron co-releasing AVP and CRF. These data suggest that AVP and CRF are co-packaged in neurosecretory vesicles and co-released into the portal capillary blood to synergistically modulate adrenocorticotropic hormone (ACTH) release from the anterior pituitary.

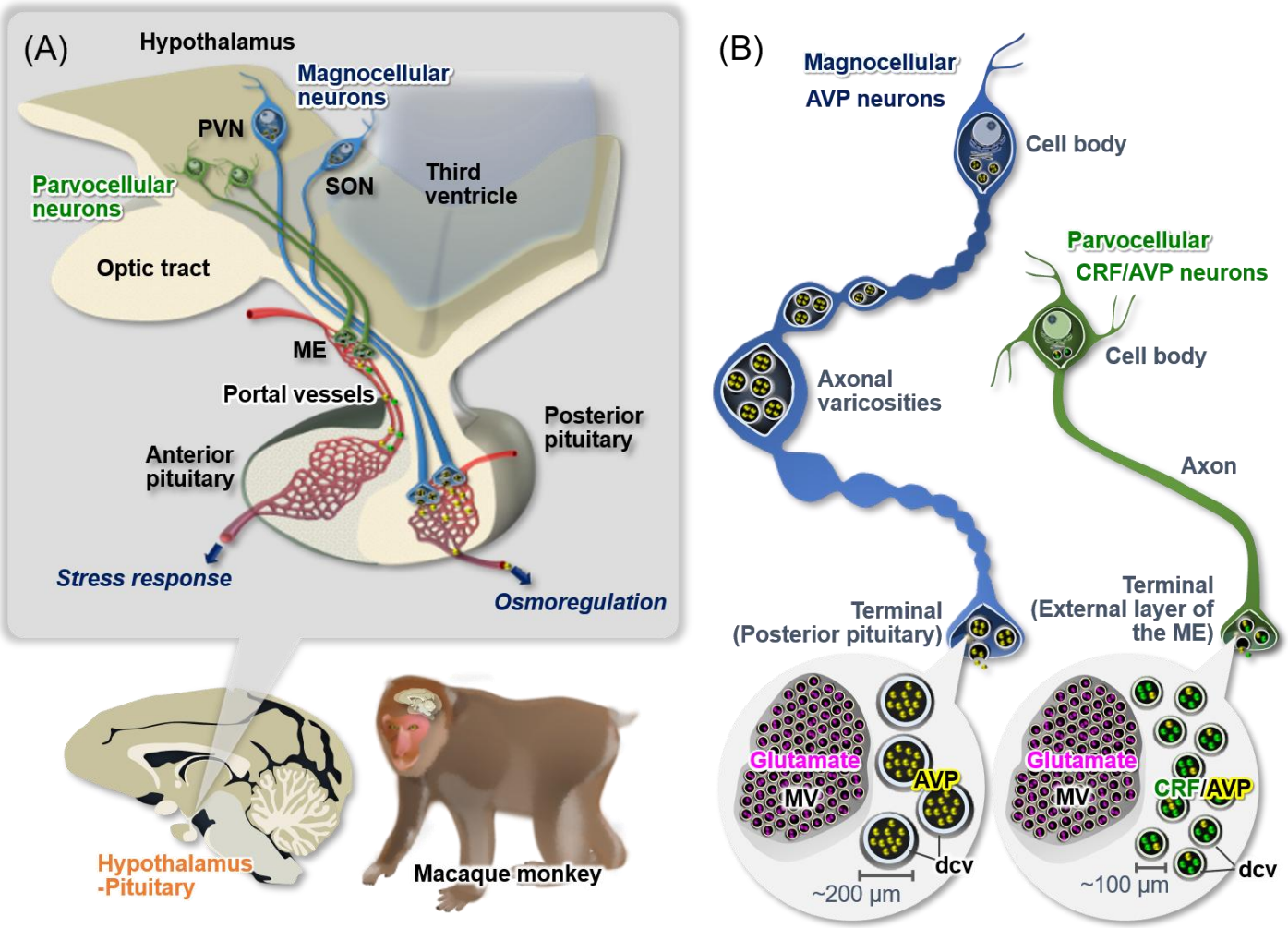

Figure GD.2 (**A**) Schematic diagram of magnocellular and parvocellular neurons in the macaque hypothalamo-pituitary axis. (**B**) Schematic diagram of magnocellular and parvocellular neuronal architecture, and of vesicle morphology in their neuronal terminals. A significant difference in dense-core vesicle (dcv) diameter was observed between magnocellular (~200 nm) and parvocellular (~100 nm) vasopressin (AVP)- and/or corticotropin-releasing factor (CRF)-producing neurons in the macaque hypothalamus. Furthermore, primate magnocellular and parvocellular AVP/CRF neurons were found to be glutamatergic. PVN, paraventricular nucleus; SON, supraoptic nucleus ME, median eminence; MV, clustered microvesicles.

Acknowledgments

I owe my deepest gratitude to my supervisor, Professor Hirotaka Sakamoto (Okayama University, Japan), for his invaluable guidance, insightful discussions, and unwavering support throughout this work. His patience and thoughtful encouragement during the more challenging phases of my graduate research were truly irreplaceable.

I am profoundly grateful to Professor Tatsuya Sakamoto, Professor Hideki Nakagoshi, and Associate Professor Takumi Oti (all at Okayama University, Japan) for their valuable comments and encouragement; I also acknowledge Professor John F. Morris (University of Oxford, UK) for his constructive feedback and suggestions. I wish to express my sincere appreciation to Assistant Professor Sho Maejima (Shimane University, Japan), Assistant Professor Keita Satoh (Kawasaki Medical School, Japan), Lecturer Yasumasa Ueda (Kansai Medical University, Japan), and Ms. Natsuko Kawakami for their expert technical assistance and generous cooperation.

Tissues of *Nihonzaru* (Japanese macaque monkeys) were provided by the National Institutes of Natural Sciences (NINS) and the Kyoto University Primate Research Institute (KUPRI) with partial support from the National Bio-Resource Project (NBRP) “Nihonzaru” of the Ministry of Education, Culture, Sports, Science and Technology (MEXT), Japan.

I would like to acknowledge the support of the Okayama University Science, Technology, and Innovation Creation Fellowship (OU Fellowship) and the Research Fellowship for Young Scientists from the Japan Society for the Promotion of Science (JSPS). Finally, I extend my heartfelt appreciation to all members of the Behavioral Neurobiology Laboratory and the Ushimado Marine Institute for their stimulating discussions, generous cooperation, and daily support−including practical assistance and thoughtful encouragement.

References

1. Walum, H. and L.J. Young, *The neural mechanisms and circuitry of the pair bond.* Nat Rev Neurosci, 2018. **19**(11): p. 643-654.
2. Buijs, R.M., et al., *Vasopressin and oxytocin: distribution and putative functions in the brain.* Prog Brain Res, 1983. **60**: p. 115-22.
3. Morris, J., *Neurosecretory Vesicles: Structure, Distribution, Release and Breakdown*, in *Neurosecretion: Secretory Mechanisms*, G. Lemons JR and Dayanithi, Editor. 2020, Springer Nature Switzerland. p. 81-102.
4. Fellmann, D., et al., *The CRF neuron: immunocytochemical study.* Peptides, 1984. **5 Suppl 1**: p. 19-33.
5. Rivier, C. and W. Vale, *Interaction of corticotropin-releasing factor and arginine vasopressin on adrenocorticotropin secretion in vivo.* Endocrinology, 1983. **113**(3): p. 939-42.
6. Vale, W., et al., *Effects of synthetic ovine corticotropin-releasing factor, glucocorticoids, catecholamines, neurohypophysial peptides, and other substances on cultured corticotropic cells.* Endocrinology, 1983. **113**(3): p. 1121-31.
7. Liu, J.H., et al., *Augmentation of ACTH-releasing activity of synthetic corticotropin releasing factor (CRF) by vasopressin in women.* J Clin Endocrinol Metab, 1983. **57**(5): p. 1087-9.
8. Fischman, A.J. and R.L. Moldow, *In vivo potentiation of corticotropin releasing factor activity by vasopressin analogues.* Life Sci, 1984. **35**(12): p. 1311-9.
9. Gillies, G.E., E.A. Linton, and P.J. Lowry, *Corticotropin releasing activity of the new CRF is potentiated several times by vasopressin.* Nature, 1982. **299**(5881): p. 355-7.
10. Murakami, K., K. Hashimoto, and Z. Ota, *Interaction of synthetic ovine corticotropin releasing factor and arginine vasopressin on in vitro ACTH release by the anterior pituitary of rats.* Neuroendocrinology, 1984. **39**(1): p. 49-53.
11. Hashimoto, K., et al., *Synergistic interaction of corticotropin releasing factor and arginine vasopressin on adrenocorticotropin and cortisol secretion in Macaca fuscata.* Acta Med Okayama, 1984. **38**(3): p. 261-7.
12. Itoi, K., et al., *Visualization of corticotropin-releasing factor neurons by fluorescent proteins in the mouse brain and characterization of labeled neurons in the paraventricular nucleus of the hypothalamus.* Endocrinology, 2014. **155**(10): p. 4054-60.

13. Mouri, T., et al., *Colocalization of corticotropin-releasing factor and vasopressin in the paraventricular nucleus of the human hypothalamus.* Neuroendocrinology, 1993. **57**(1): p. 34-9.
14. Whitnall, M.H., E. Mezey, and H. Gainer, *Co-localization of corticotropin-releasing factor and vasopressin in median eminence neurosecretory vesicles.* Nature, 1985. **317**(6034): p. 248-50.
15. Vale, W., et al., *Characterization of a 41-residue ovine hypothalamic peptide that stimulates secretion of corticotropin and beta-endorphin.* Science, 1981. **213**(4514): p. 1394-7.
16. Shibahara, S., et al., *Isolation and sequence analysis of the human corticotropin-releasing factor precursor gene.* EMBO J, 1983. **2**(5): p. 775-9.
17. Rivier, J., J. Spiess, and W. Vale, *Characterization of rat hypothalamic corticotropin-releasing factor.* Proc Natl Acad Sci U S A, 1983. **80**(15): p. 4851-5.
18. Whitnall, M.H., *Regulation of the hypothalamic corticotropin-releasing hormone neurosecretory system.* Prog Neurobiol, 1993. **40**(5): p. 573-629.
19. Bartanusz, V., et al., *Stress-induced increase in vasopressin and corticotropin-releasing factor expression in hypophysiotrophic paraventricular neurons.* Endocrinology, 1993. **132**(2): p. 895-902.
20. Tilders, F.J., E.D. Schmidt, and D.C. de Goeij, *Phenotypic plasticity of CRF neurons during stress.* Ann N Y Acad Sci, 1993. **697**: p. 39-52.
21. Land, H., et al., *Nucleotide sequence of cloned cDNA encoding bovine arginine vasopressin-neurophysin II precursor.* Nature, 1982. **295**(5847): p. 299-303.
22. Davies, J., et al., *Further delineation of the sequences required for the expression and physiological regulation of the vasopressin gene in transgenic rat hypothalamic magnocellular neurones.* J Neuroendocrinol, 2003. **15**(1): p. 42-50.
23. Breslow, E., *Structure and folding properties of neurophysin and its peptide complexes: biological implications.* Regul Pept, 1993. **45**(1-2): p. 15-9.
24. Breslow, E., *Chemistry and biology of the neurophysins.* Annu Rev Biochem, 1979. **48**: p. 251-74.
25. Morgenthaler, N.G., et al., *Copeptin: clinical use of a new biomarker.* Trends Endocrinol Metab, 2008. **19**(2): p. 43-9.
26. Bao, A.M. and D.F. Swaab, *Corticotropin-releasing hormone and arginine vasopressin in depression focus on the human postmortem hypothalamus.* Vitam Horm, 2010. **82**: p. 339-65.

27. Plotsky, P.M. and P.E. Sawchenko, *Hypophysial-portal plasma levels, median eminence content, and immunohistochemical staining of corticotropin-releasing factor, arginine vasopressin, and oxytocin after pharmacological adrenalectomy.* Endocrinology, 1987. **120**(4): p. 1361-9.
28. Satoh, K., et al., *In vivo processing and release into the circulation of GFP fusion protein in arginine vasopressin enhanced GFP transgenic rats: response to osmotic stimulation.* FEBS J, 2015. **282**(13): p. 2488-99.
29. Rehbein, M., et al., *The neurohypophyseal hormones vasopressin and oxytocin. Precursor structure, synthesis and regulation.* Biol Chem Hoppe Seyler, 1986. **367**(8): p. 695-704.
30. Hara, Y., J. Battey, and H. Gainer, *Structure of mouse vasopressin and oxytocin genes.* Brain Res Mol Brain Res, 1990. **8**(4): p. 319-24.
31. Wang, H., A.R. Ward, and J.F. Morris, *Oestradiol acutely stimulates exocytosis of oxytocin and vasopressin from dendrites and somata of hypothalamic magnocellular neurons.* Neuroscience, 1995. **68**(4): p. 1179-88.
32. Castel, M., et al., *Improved visualization of the immunoreactive hypothalamo-neurohypophysial system by use of immuno-gold techniques.* Cell Tissue Res, 1986. **243**(1): p. 193-204.
33. Sawchenko, P.E., L.W. Swanson, and W.W. Vale, *Co-expression of corticotropin-releasing factor and vasopressin immunoreactivity in parvocellular neurosecretory neurons of the adrenalectomized rat.* Proc Natl Acad Sci U S A, 1984. **81**(6): p. 1883-7.
34. Foote, S.L. and C.I. Cha, *Distribution of corticotropin-releasing-factor-like immunoreactivity in brainstem of two monkey species (Saimiri sciureus and Macaca fascicularis): an immunohistochemical study.* J Comp Neurol, 1988. **276**(2): p. 239-64.
35. Shaw, F.D., M. Castel, and J.F. Morris, *Ultrastructural characterisation of vasopressinergic terminals in the lateral septum of murine brains by use of monoclonal anti-neurophysins.* Cell Tissue Res, 1987. **249**(2): p. 403-10.
36. Kawata, M. and Y. Sano, *Immunohistochemical identification of the oxytocin and vasopressin neurons in the hypothalamus of the monkey (Macaca fuscata).* Anat Embryol (Berl), 1982. **165**(2): p. 151-67.
37. Kawata, M., et al., *Immunohistochemical demonstration of corticotropin releasing factor containing nerve fibers in the median eminence of the rat and monkey.* Histochemistry, 1982. **76**(1): p. 15-9.

38. Zimmerman, E.A., et al., *Vasopressin and neurophysin: high concentrations in monkey hypophyseal portal blood.* Science, 1973. **182**(4115): p. 925-7.
39. Raadsheer, F.C., et al., *Localization of corticotropin-releasing hormone (CRH) neurons in the paraventricular nucleus of the human hypothalamus; age-dependent colocalization with vasopressin.* Brain Res, 1993. **615**(1): p. 50-62.
40. Hook, V., et al., *Proteases for processing proneuropeptides into peptide neurotransmitters and hormones.* Annu Rev Pharmacol Toxicol, 2008. **48**: p. 393-423.
41. Dong, W., et al., *Cellular localization of the prohormone convertases in the hypothalamic paraventricular and supraoptic nuclei: selective regulation of PC1 in corticotrophin-releasing hormone parvocellular neurons mediated by glucocorticoids.* J Neurosci, 1997. **17**(2): p. 563-75.
42. Wagner, C.K. and L.G. Clemens, *Neurophysin-containing pathway from the paraventricular nucleus of the hypothalamus to a sexually dimorphic motor nucleus in lumbar spinal cord.* J Comp Neurol, 1993. **336**(1): p. 106-116.
43. Wagner, C.K. and L.G. Clemens, *Projections of the paraventricular nucleus of the hypothalamus to the sexually dimorphic lumbosacral region of the spinal cord.* Brain Res, 1991. **539**(2): p. 254-262.
44. Hallbeck, M. and A. Blomqvist, *Spinal cord-projecting vasopressinergic neurons in the rat paraventricular hypothalamus.* J Comp Neurol, 1999. **411**(2): p. 201-11.
45. Castel, M. and J.F. Morris, *The neurophysin-containing innervation of the forebrain of the mouse.* Neuroscience, 1988. **24**(3): p. 937-66.
46. Otubo, A., et al., *Vasopressin gene products are colocalised with corticotrophin-releasing factor within neurosecretory vesicles in the external zone of the median eminence of the Japanese macaque monkey (Macaca fuscata).* J Neuroendocrinol, 2020. **32**(8): p. e12875.
47. Kawakami, N., et al., *Variation of pro-vasopressin processing in parvocellular and magnocellular neurons in the paraventricular nucleus of the hypothalamus: Evidence from the vasopressin-related glycopeptide copeptin.* J Comp Neurol, 2021. **529**: p. 1372-1390.
48. Abbott, A., *Biomedicine: the changing face of primate research.* Nature, 2014. **506**(7486): p. 24-6.
49. Koshimizu, T.A., et al., *Vasopressin V1a and V1b receptors: from molecules to physiological systems.* Physiol Rev, 2012. **92**(4): p. 1813-64.

50. Meeker, R.B., et al., *Ultrastructural distribution of glutamate immunoreactivity within neurosecretory endings and pituicytes of the rat neurohypophysis.* Brain Res, 1991. **564**(2): p. 181-93.
51. Meeker, R.B., D.J. Swanson, and J.N. Hayward, *Light and electron microscopic localization of glutamate immunoreactivity in the supraoptic nucleus of the rat hypothalamus.* Neuroscience, 1989. **33**(1): p. 157-67.
52. Valentino, R.J., et al., *Corticotropin-releasing factor is preferentially colocalized with excitatory rather than inhibitory amino acids in axon terminals in the peri-locus coeruleus region.* Neuroscience, 2001. **106**(2): p. 375-84.
53. Maunsbach, A.B., *The influence of different fixatives and fixation methods on the ultrastructure of rat kidney proximal tubule cells. II. Effects of varying osmolality, ionic strength, buffer system and fixative concentration of glutaraldehyde solutions.* J Ultrastruct Res, 1966. **15**(3): p. 283-309.
54. Maunsbach, A.B., *The influence of different fixatives and fixation methods on the ultrastructure of rat kidney proximal tubule cells. I. Comparison of different perfusion fixation methods and of glutaraldehyde, formaldehyde and osmium tetroxide fixatives.* J Ultrastruct Res, 1966. **15**(3): p. 242-82.
55. Sun, D., A.J. Vingrys, and M. Kalloniatis, *Metabolic and functional profiling of the normal rat retina.* J Comp Neurol, 2007. **505**(1): p. 92-113.
56. Balaram, P., T.A. Hackett, and J.H. Kaas, *Differential expression of vesicular glutamate transporters 1 and 2 may identify distinct modes of glutamatergic transmission in the macaque visual system.* J Chem Neuroanat, 2013. **50-51**: p. 21-38.
57. Cannata, M.A. and J.F. Morris, *Changes in the appearance of hypothalamo-neurohypophysial neurosecretory granules associated with their maturation.* J Endocrinol, 1973. **57**(3): p. 531-8.
58. Ziegler, D.R., W.E. Cullinan, and J.P. Herman, *Distribution of vesicular glutamate transporter mRNA in rat hypothalamus.* J Comp Neurol, 2002. **448**(3): p. 217-29.
59. Zhang, L., et al., *VGLUT-VGAT expression delineates functionally specialised populations of vasopressin-containing neurones including a glutamatergic perforant path-projecting cell group to the hippocampus in rat and mouse brain.* J Neuroendocrinol, 2020. **32**(4): p. e12831.
60. Hrabovszky, E. and Z. Liposits, *Glutamatergic phenotype of hypothalamic neurosecretory systems: a novel aspect of central neuroendocrine regulation.* Ideggyogy Sz, 2007. **60**(3-4): p. 182-6.

61. Brann, D.W., *Glutamate: a major excitatory transmitter in neuroendocrine regulation.* Neuroendocrinology, 1995. **61**(3): p. 213-25.
62. Hrabovszky, E., et al., *Localization and osmotic regulation of vesicular glutamate transporter-2 in magnocellular neurons of the rat hypothalamus.* Neurochem Int, 2006. **48**(8): p. 753-61.
63. Naugle, M.M., et al., *Age and Long-Term Hormone Treatment Effects on the Ultrastructural Morphology of the Median Eminence of Female Rhesus Macaques.* Neuroendocrinology, 2016. **103**(6): p. 650-64.
64. Holmes, R.L., *Comparative Observations on Inclusions in Nerve Fibres of the Mammalian Neurohypophysis.* Z Zellforsch Mikrosk Anat, 1964. **64**: p. 474-92.
65. Armstrong, W.E. and M. Tian, *Separate ultrastructural distributions of neurophysin and C-terminal glycopeptide within dense core vesicles in rat neural lobe.* Brain Res, 1991. **562**(1): p. 144-8.
66. Morris, J.F., *Hormone storage in individual neurosecretory granules of the pituitary gland: A quantitative ultrastructural approach to hormone storage in the neural lobe.* J Endocrinol, 1976. **68**(02): p. 209-224.
67. Frahm, S., et al., *An essential role of acetylcholine-glutamate synergy at habenular synapses in nicotine dependence.* Elife, 2015. **4**: p. e11396.
68. Mills, F., et al., *Cadherins mediate cocaine-induced synaptic plasticity and behavioral conditioning.* Nat Neurosci, 2017. **20**(4): p. 540-549.
69. Hou, S., et al., *Plasticity of lumbosacral propriospinal neurons is associated with the development of autonomic dysreflexia after thoracic spinal cord transection.* J Comp Neurol, 2008. **509**(4): p. 382-99.